# Development of Platform Independent Remote Experiments

A Thesis

Presented to

The Faculty of the Department of Mechanical Engineering

University of Houston

In Partial Fulfillment

Of the Requirements for the Degree

Master of Science

In Mechanical Engineering

by

Jun Weng

May 2014

**Development of Platform Independent Remote Experiments**

_____

Jun Weng

Approved:

Chair of the Committee
Gangbing Song, Professor
Department of Mechanical Engineering

Committee Members:

Li Sun, Associate Professor
Department of Mechanical Engineering

Xuemin Chen, Associate Professor
Department of Engineering Technology
College of Science and Technology
Texas Southern University

Siu Chun Michael Ho, Ph. D.
Department of Mechanical Engineering

Suresh Khator, Associate Dean,
Cullen College of Engineering

Pradeep Sharma, Chairman
Department of Mechanical Engineering

## Acknowledgements

I want to gratefully thank my advisor Dr. Gangbing Song for mentoring me and supporting my thesis studies technically and financially in Smart Material and Structure Laboratory. I am grateful that Dr. Song provided me an opportunity to set up a remote laboratory at Texas A&M University at Qatar. I am very thankful to him for his time and concerns on my studies. I could not finish my thesis without his help and suggestions.

I want to thank Dr. Xuemin Chen, Dr. Hamid R. Parsaei, and Dr. Song again. Dr. Chen went with Mr. Ning Wang from TSU and helped us fit into new culture and new environment in Qatar in the first week. Dr. Chen and Dr. Song had many teleconferences with the Dr. Hamid R. Parsaei in TAMUQ to help us set up the remote laboratory. I could not finish my work presented in this thesis if I did not receive such great help from them.

I want to thank Dr. Siu Chun Michael Ho who provided helpful suggestions on my thesis and Mr. Ning Wang who worked with me in this project. I want to thank others who helped me on my studies and thesis, Ms. Trina Johnson, Dr. Claudio Olmi, Mr. Daniel Osakue, Mr. Shujun Yang, Mr. Devendra Patil, Mr. Yasser Al-Hamidi (TAMUQ), all SMSL students, and my very supporting families. All of them were great and very helpful along the way of my thesis work. At the last, I want to thank Qatar Foundation's National Priorities Research Program (NPRP) for their funding, so I can work on the project NPRP 4-891-2-335: Hands-on Experiment via Internet – To develop a Unified Remote Laboratory Framework for Cross Nation Engineering Education.

# Development of Platform Independent Remote Experiments

An Abstract

of a

Thesis

Presented to

the Faculty of the Department of Mechanical Engineering

University of Houston

In Partial Fulfillment

of the Requirements for the Degree

Master of Science

in Mechanical Engineering

by

Jun Weng

May 2014

# Abstract

Remote laboratory or online laboratory is the use of the Internet to conduct real experiments remotely when the client is geographically away from the real experiments. Current remote laboratories such as the remote laboratory in Mechanical Engineering at University of Houston require the client to install plug-ins before conducting remote experiments. This thesis presents an advanced technology using JavaScript and Socket.IO to develop plug-in free remote experiments without firewall issue. A scalable plug-in free remote laboratory integrated with two remote experiments has been set up in the Mechanical Engineering Department at the Texas A&M University at Qatar (TAMUQ) in Qatar under the collaboration from the University of Houston and the Texas Southern University in Houston, Texas. The plug-free remote laboratory has been successfully tested in Windows PC, Mac OS, iPhone and iPad (iOS).

# Table of Contents

# List of Figures

# List of Tables

# Chapter 1 Introduction

## 1.1 Motivation and Objectives

Since the invention of the Internet in the 1970s, distance learning has become a growing trend in the education community. Remote laboratory as a method of distance learning for science and engineering has been widely researched since the late 1990s. A remote laboratory is characterized by the use of telecommunication technology to conduct experiments remotely when the client is geographically away from the physical experiments [1], [19]. In the past 15 years, remote laboratories have been used to assist teaching in different subjects. Students who had used remote laboratories in their courses found that remote laboratories helped them understand course materials better [2], [3], [4].

Most currently active remote laboratories, such as a remote laboratory in Smart Materials and Structures Laboratory (SMSL) in the Department of Mechanical Engineering at the University of Houston (UH), require the client to install plug-ins in order to conduct the remote experiments. The remote laboratory in SMSL requires the user to install National Instrument (NI) Laboratory Virtual Instrument Engineering Workbench (LabVIEW) run-time engine in the client's PC to use the remote panel to conduct the experiment and ActiveX to view real-time streaming videos. The requirement for plug-ins limits the accessibility and usability of the remote laboratory. For example, consider a client who has downloaded and installed two plug-ins, the LabVIEW run-time engine, and ActiveX in his first PC; but the client forgot his first PC at home and now needs to conduct a remote experiment for his homework assignment. In this case, the client must install the plug-ins again in another PC which may belong to his friend or is a public library computer (may not allow installation of plug-ins). Although the plug-ins

have been installed in the second PC, the remote experiment is not guaranteed to work in that PC at the first time. According to the history of the clients in UH using the remote laboratory in related courses, each semester several students report that they could not conduct the remote experiments even though plug-ins had been installed successfully in their PCs, or that the setting in computer took them too much time to conduct the remote experiment successfully. Furthermore remote laboratories that require plug-ins may result in firewall issues depending on the way the remote laboratories are developed. For example, real-time cameras for remote experiments in the SMSL at the UH use port 7000 and 8000 for video streaming. Using these ports for public access can result in network safety issues from hackers. In some universities, the IT department prohibits university computers from opening other ports except port 80 to preserve network safety.

Under the motivation of allowing users to conduct experiments anywhere and anytime without installation of plug-ins and running into firewall issue, an advanced technology will be developed to solve these problems. This thesis has the following five objectives:

1) Develop plug-in free user interface to conduct remote experiments and view the experiments through a real-time camera;

2) Ensure that remote experiments are safe and secure enough to pass firewalls;

3) Ensure that remote experiments are compatible with any operating system and any devices including smart phones and tablets;

4) Integrate a remote laboratory with multiple experiments for the users to interact with;

5) Collaborate with Texas Southern University and Texas A&M University at Qatar (TAMUQ) to set up a plug-in free remote laboratory in the Mechanical Engineering Department at TAMUQ.

## 1.2 Contribution and Significance

An advanced technology is presented in this thesis to make a plug-in free remote laboratory possible. The technology uses pure JavaScript to develop the plug-in free remote laboratory. A remote laboratory based on JavaScript passes firewall security safely and securely. The advanced technology contains two parts, a part between Internet server and local experiments, and the other part between Internet server and web browser. This work is a collaboration with the Texas Southern University and the Texas A&M University at Qatar.

The first part of the solution technology between the Internet server and the local experiment fulfills objectives one through three. The solution uses a module named LabVIEW to Node.js (LtoN) based on JSON Toolkit released by NI for LabVIEW and improved by the development team for the use in remote experiments. The server is developed using Socket.IO which is a JavaScript library and the server can only read and send data in JSON format. The LtoN module in LabVIEW decodes the command sent from the server and encodes the data to send from LabVIEW to the server in JSON format, which is recognized by the server.

The solution for the part of the communication between the server and the client's web browser was mainly contributed by Mr. Ning Wang of TSU. This part uses Socket.IO technology for the development of a JavaScript based user interface. This part of the technology also fulfills objectives one through three.

A remote laboratory at TAMUQ with the advanced technology fulfilling objectives four and five has been set up. The remote laboratory was integrated with the Shape Memory Alloy experiment and the Smart Vibration Platform experiment to help the engineering students in Mechanical Engineering Department at TAMUQ learning related topics. The plug-in free remote laboratory has been successfully tested in multiple operating systems, including Microsoft Windows, Mac OS, and Apple iOS (iPhone and iPad).

## 1.3 Thesis Organization

This thesis consists of six chapters. Chapter one discusses the motivation, objectives, contribution, and significance of the study. An advanced technology is desired for plug-in free remote experiments and remote laboratory. The plug-in free remote laboratory is also safe and secure to pass the firewall.

Chapter two covers a literature review on remote laboratories and nonlinear control of Shape Memory Alloys (SMA). The state of the art of remote laboratories is also covered in this chapter. There are brief introductions of several well-developed remote laboratories in the world. There is also an introduction to the remote Smart Vibration Platform (SVP) experiment which is related to the remote laboratory set up at the TAMUQ.

Chapter three introduces what smart materials are. There are discussions about two important class of smart materials, SMA and Magneto-Rheological (MR) fluids, which are used by the two remote experiments in the remote laboratory at the TAMUQ.

Chapter four presents a remote experiment using SMA, called SMA experiment. It introduces the experimental setup of the SMA device, the programming for the

experimental control in National Instruments (NI) Virtual Instrument Engineering Workbench (LabVIEW), and the results of the experiment. It also discusses the implementation of Pulse Width Modulation (PWM) method and the sliding mode based nonlinear displacement control of SMA in the SMA experiment.

Chapter five discusses the novel remote laboratory set up at TAMUQ by using the advanced technology. The result of conducting SMA experiment using the plug-in free remote panel is presented. There is also a comparison between the regular remote panel from the Web Publishing tool in the LabVIEW and our novel remote laboratory.

Chapter six concludes the work presented in this thesis. A remote laboratory has been set up at the TAMUQ with two remote experiments ready to use. The future work is also discussed in this chapter.

# Chapter 2 Literature Review

## 2.1 Remote Laboratory

### 2.1.1 Introduction

With the development of the Internet, many innovations are invented to directly or indirectly benefit the life and the education. In the engineering education community, remote laboratory (a.k.a online laboratory or remote workbench) becomes very popular among schools and universities in the world.

Remote laboratory has discovered to have many advantages. Many institutes and universities use remote laboratories to save money and share sources with other institutes. Due to the time cost by allowing students having access to the lab equipment, the deployment of remote laboratories can efficiently solve this problem. The students may also access the laboratory anytime and anywhere. In comparison to the traditional laboratories, the hours of the building open and the working schedule of the staff in the laboratory would become a problem of preventing students to use the lab; however, the remote laboratory can solve these issues. Remote laboratories have many more benefits.

### 2.1.2 State of the Art about Remote Laboratories

Remote laboratory is not a new concept nowadays. Since the invention of the Internet in 1970s, e-learning becomes a new topic in the education community. Remote laboratory as one of e-learning methods helps the students to learn their subject better. The development of remote laboratories started in late 1990s. According to [5] there were a peak around 2002/2003 and another one around 2006 for the number of publications. Based on the recent literature search performed using the database provided by the library in University of Houston, the number of publications related to remote laboratory keeps

increasing. The keywords used in the search are "remote lab", "remote experiments*", "online lab*", and "virtual lab*" where "*" is for wildcards. The results are shown in Table 2-1 and plotted in Figure 2-1.

**Table 2-1:** Results of literature search about remote laboratory related keywords in University of Houston library database

| Year | Number of Results |
|---|---|
| 1998-1999 | 294,093 |
| 1999-2000 | 347,355 |
| 2000-2001 | 375,731 |
| 2001-2002 | 383,052 |
| 2002-2003 | 413,826 |
| 2003-2004 | 472,078 |
| 2004-2005 | 557,370 |
| 2005-2006 | 646,490 |
| 2006-2007 | 724181 |
| 2007-2008 | 796517 |
| 2008-2009 | 850,891 |
| 2009-2010 | 889,134 |
| 2010-2011 | 972,254 |
| 2011-2012 | 996,041 |
| 2012-2013 | 930,228 |

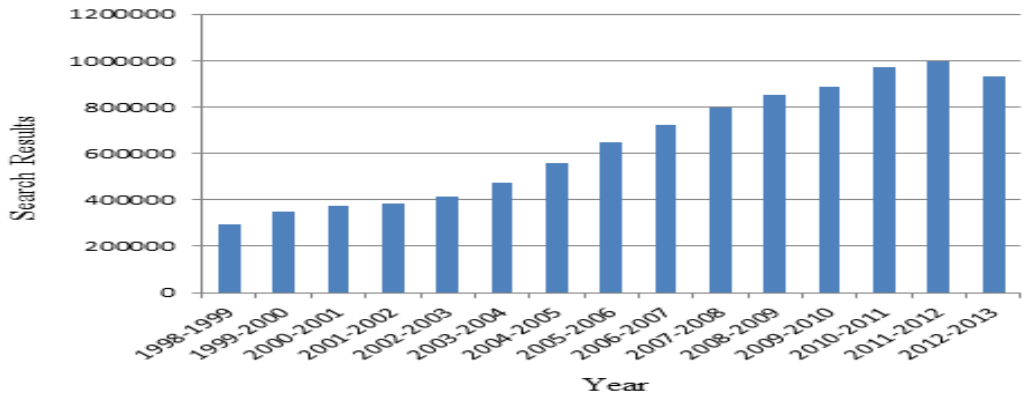


**Figure 2-1:** Plot for the results of literature search about remote laboratory related keywords in University of Houston library database

We can see from Table 2-1 and Figure 2-1 that remote laboratory has been developed for a quite long time and the peak period was from 2002 to 2011; however, the number of publication decreased in recent two to three years. This is an interesting phenomenon.

Many remote laboratories have been set up based on various and different technologies such as Java, MATLAB/Simulink, LabVIEW, and C/C++. That increase the possibility of remote laboratories, but the variety also makes the reusability and cooperation among different remote laboratories very difficult. That difficulty could also be a bottleneck and challenge for the development of remote laboratory [5].

The technologies used in the development of remote laboratories are various. In the past 15 years of the development of remote laboratories, MATLAB/Simulink and LabVIEW are the major software used for the development of experiment environment. The server majorly uses Apache in Linux and Microsoft IIT in Microsoft Operation System. MySQL and Microsoft SQL are the most widely used database since late 1990s. Java, HTML, and JavaScript, PHP, and Adobe Flash are all popular choices for the development of graphical user interface (GUI). The real-time video uses ActiveX as the majority. Figure 2-2 depicts a time line of technology development in remote laboratory based on public information and references [5]-[15].

Most major software and technologies found in recent laboratories were from 2000 and earlier. According to literature and public information, there are at least four new technologies (the results may not represent all remote laboratories) found in recent remote laboratories. In 2004, Easy Java Simulations (EJS) was released. In 2005, a remote laboratory presented in [7] used EJS for the development for Graphical User Interface (GUI). In 2006, Asynchronous JavaScript and XML (Ajax) was released. In 2008, iLab by MIT successfully adopted Ajax in the development of GUI [6]. In 2009, Adobe Flash was released and adopted for the use in GUI in remote laboratory at the same year [7]. Red 5 is an open-source media streaming server whose Version 1.0 was

release in December, 2012. Two years later, Red 5 has been found being used for real-time video in remote laboratory [10].

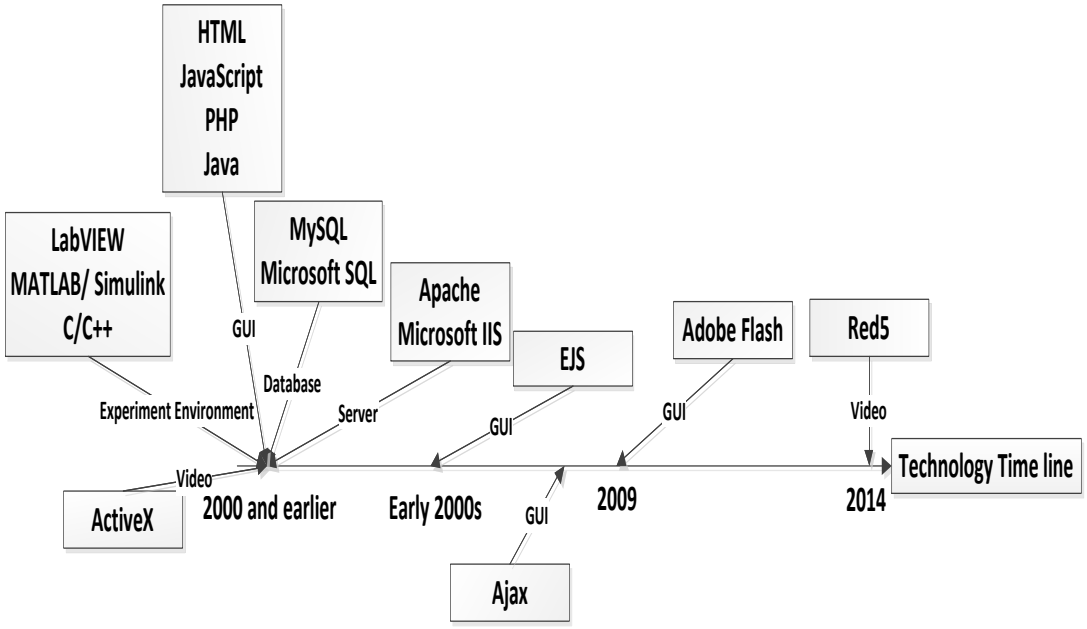


**Figure 2-2:** Time line of technology development in remote laboratory

The classification of remote laboratories is dependent. Remote laboratories in the world are developed depending on different technologies. We can classify them by four aspects in the following. There is no certain law to follow to classify remote laboratories. Thus, this way of classification only represents the author's view based on general review about the topic.

*Experiment*

From review of the past remote laboratories, MATLAB/Simulink and LabVIEW are the most two major software used in the programming of the experiment. For examples, iLab uses LabVIEW to program the experiments [6], a remote laboratory set up at Slovak University of Technology uses MATLAB to program the experiment and Java to decode the data in the server [7], and more remote laboratories using

LabVIEW in [14], [15]. The rest of the experiments use other programming language such as C/C++ and Python.

*Web Servers and Database*

Because of limited options, a web server can run Apache, Microsoft IIS or others for the Web interface. The database can use MySQL, Microsoft SQL, Oracle or others. For examples, a remote laboratory at the University of Texas at San Antonio, TX, USA uses Ubuntu Linux system, Apache HTTM for the Web interface, and MySQL for the database [10]. As reference to MIT iCampus iLabs Software Architecture Workshop by P. Bailey on June 13-15, 2006, the lab server in MIT iCampus iLabs built on Windows using .NET Framework (Internet Information Services, IIS) and Microsoft SQL for database [11].

*Server/Client*

The server has two types, Client-Server (CS) and Browser-Server (BS), for remote laboratories. CS means the server is on the client's machine and BS means the server is on the browser. In CS remote laboratories, clients need to install extra software to helps the client connect to the server. For an example, conventional remote laboratories such as the remote laboratory at the UH use LabVIEW remote panel created by Web Publishing Tool by NI. In order to run the remote panel, the client has to install run-time engine to communicate with the server, although the remote panel is embedded in an HTML page. BS remote laboratories have no requirement about installing additional software to connect with the server, but only plug-ins to run the user interface. The new remote laboratory developed at TAMUQ is an example of BS remote laboratory. Any devices and any system can conduct the

remote laboratory at TAMUQ by only using a browser.

*Graphical User Interface (GUI)*

No matter in CS or BS remote laboratory, they all use various technologies to design GUI. Popular interface options are Flash, Java Applets, ActiveX, JavaScript and HTML, etc.

**Table 2-2:** Dependent ways of classifying remote laboratories

| | Classification |
|---|---|
| Experiment | - Visual programming: MATLAB/Simulink, LabVIEW<br>- Programming Languages: C/C++, Python |
| Web Servers | -Apache<br>-Microsoft IIS for Windows NT family<br>… |
| Database | -MySQL<br>-Microsoft SQL<br>-Oracle<br>… |
| Server/Client | - Client-Server<br>- Browser-Server |
| Graphical User Interface | - Flash<br>- Java Applets<br>- ActiveX<br>- JavaScript<br>- HTML<br>… |

Many institutes had deployed remote laboratories for the educational purposes such as MIT iCampus iLab [6], Labshare using open source SAHARA system [13], and Lila Booking System [12]. A general review about these developed remote laboratories is helpful to better introduce the state of the art of remote laboratory.

*MIT iCampus iLab*

MIT iCampus iLab is a bundle of remote laboratories around the world. iLab project started as the iCampus project (1999 to 2006) between MIT and Microsoft by

del Alamo and his collegues. iLab first came out to explore the potential of online laboratories to benefit the education of undergrad students. By 2008, iLab had been expanded to nine countries and used by 5400 students [6]. From the website of iLab MIT, the latest update of their activities was in July 2011. iLab is built on Windows using .NET Framework (Internet Information Services, IIS) and Microsoft SQL for database [11]. The experiments of iLab use LabVIEW in programming, which makes iLab CS a remote laboratory.

*LabShare*

LabShare is a remote laboratory shared by four universities in Australia with a mission to build leading remote laboratories (www.labshare.edu.au). The users have access to all remote experiments shared by the four universities. In the control of the remote laboratory, the users can drag the camera to the position they want to view and control the experiment through a web based GUI. According to [13] the GUI is developed using Asynchronous JavaScript and XML (AJAX).

*LiLa Booking System*

LiLa (Library of Labs) started by eight universities and three enterprises (www.lila-project.org). According to [12] and [23], Lila has been widely contributes to Europe by helping students to schedule remote laboratories using the booking system. LiLa's remote experiments are built using LabVIEW. In order to run the remote experiments, the users need to install LabVIEW 8.2 run-time engine. The client's web browser (GUI) uses JavaScript, sometimes Java or Flash. The server uses Windows system with Microsoft SQL and Visual Studio .NET or NETLab.

### 2.1.3 Development of the Framework of the Remote Laboratory at the University of Houston and Texas Southern University

A remote laboratory has already been developed in the Smart Materials and Structures Laboratory (SMSL) at the University of Houston (UH) [20]. The remote laboratory in SMSL has a scalable framework, which means more remote experiments can be added to the remote laboratory. We are also using this scalable framework to develop our novel remote laboratory at TAMUQ. The novel remote laboratory at TAMUQ will have more advantages like plug-in free, which we will discuss more in later chapters.

The remote laboratory system in SMSL connects several physical experiments with clients in the Internet using a Scheduler Web Server (SWS) to manage, authenticate and schedule clients and experiments. Fig. 2-3 [20] depicts a simplified framework for a scalable remote laboratory. The SWS for the remote laboratory in the Mechanical Engineering Department at the UH is using Apache web server in a Linux computer. The generation of HTML pages uses PHP and MySQL. The address, http://rsmsl-1.me.uh.edu, links to the website of the Remote Smart Materials and Structure Laboratory (RSMSL).

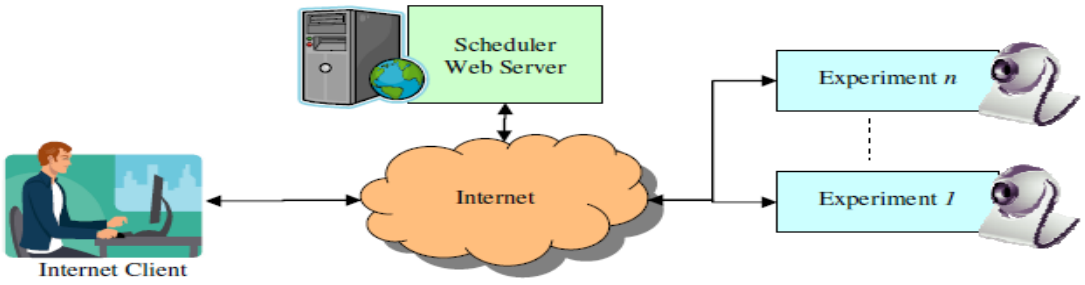


**Figure 2-3:** Simplified framework for a scalable remote laboratory

In the aim the client can use desktops and laptops with any web browser and operating system to use the remote laboratory; however, it would require lots of work to

develop such a remote laboratory [25]. Therefore, the client can only use the major web browsers like Internet Explorer, Mozilla Firefox, Apple Safari, and Google Chrome. The major operating system includes Microsoft Windows, Apple OSX, and Linux.

The physical experiments use National Instrument (NI) LabVIEW for their development. The clients need to install LabVIEW run-time engine in their laptop or computer in order to conduct the experiments in the remote laboratory. The version of the run-time engine is the same as the version of the LabVIEW used in the development of the experiment which should be given by the developer. For example, the run-time engine 2011 is not compatible to the remote experiment if the development of the experiment uses LabVIEW 2012. Besides of the run-time engine, the clients should have at least 1Mbit/sec Internet speed to conduct the remote experiments.

The Internet clients and physical experiment one to physical experiment n are connected through the Internet; at the same time, they are managed by the SWS. The clients with authorized login information are able to schedule an experiment through the scheduler. When the scheduled time comes, buttons in the webpage becomes visible which directly link to the scheduled experiment control panel and real-time camera. A countdown clock is visible to the clients to notify them the available remaining time to conduct the experiment. The maximum time is one hour. If they need more time, the clients can schedule another session. It limits the time of using the experiment of the clients, but it ensures equal chances to conduct the experiments for every client.

The SWS allows the experiments in the same sub network of the server or different. It allows the remote laboratory to become a farm of remote experiments at different locations. The remote laboratory in SMSL has several experiments for educational

purposes integrated in the system. It has been found that the in class demonstration helps the student's learning experience [22]. Such remote laboratories has been developed and put into use in the teaching of vibration and controls in Dr. Gangbing Song's classes in the UH [21] and engineering technology education in Texas Southern University (TSU)[24].

The SWS system uses authentication technique to allow the remote laboratory to work in a managed and secured environment. When the scheduled time comes, the experiment becomes available to the client who has scheduled an experiment. The client can use the buttons in the webpage to link to the experimental control panel and the real-time video page. The linking URL is under the protection using the user/experiment authorization technique as shown in Fig. 2-4 [20], where the REE is Remote Experiment Engine. The REE is the software to perform all the tasks dealing with the client, the experiment server and the SWS. To prevent a fake URL and ensure the performance of the scheduler system, the REE sends requested user's ID to the SWS to compare with the scheduled user's ID. If the IDs are the same, the REE sends a valid front panel to the client [24]. The client can have up to one hour to conduct the experiment and view the experiment through the real-time video.

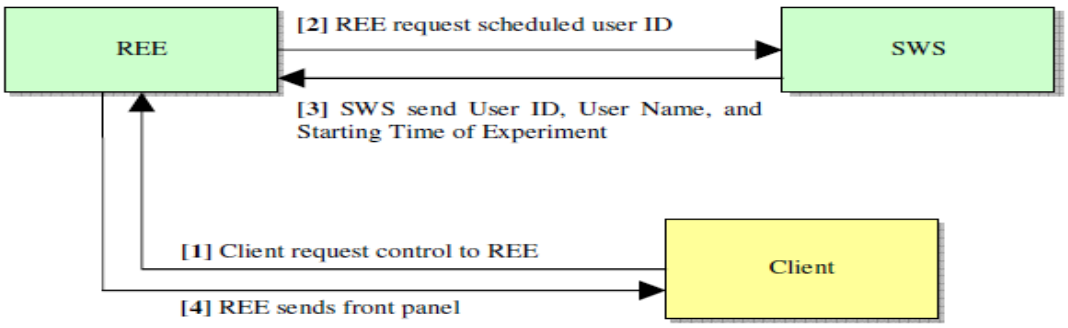


**Figure 2-4:** User/experiment authorization block diagram

The remote laboratory website has a feature of saving data and managing the data files saved by the clients to let the clients perform further analysis and work on research or homework [20]. The saved data is available for downloading from the website. The clients are able to download all the data they have saved in every experiment and they can delete the data files in the database if some are no longer useful. The SWS stores the data files in one folder and the files are linked to the user ID using a MySQL database table [20].

After the data has been saved in the SWS, Fig. 2-5 [20] depicts how the REE recalls the saved data file from the SWS. The REE sends request with the user's ID to the SWS, the SWS starts downloading and links the user's ID and the experiment ID with the saved files in the database. The downloaded files are saved in ".csv" that the client can open the file in Microsoft Excel or Notepad. The file name is related to the date and time when the data is recorded.

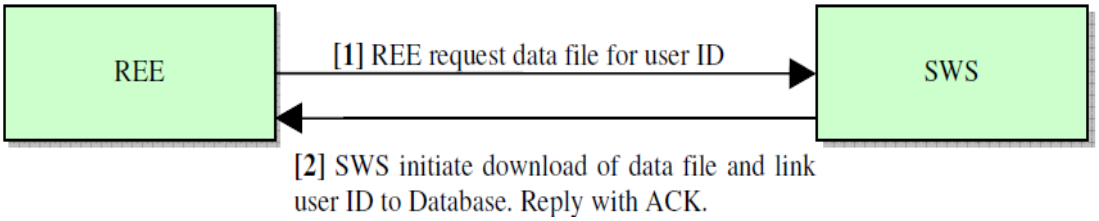


**Figure 2-5:** Data file saving block diagram

The database uses MySQL software to manage clients, experiment, and data files. MySQL software provides high performance in comparison to other database packages, which is necessary in case that the number of clients will increase in the future [20]. The database supports the 8-bit uniform transformation format (UTF8) character encoding for being compatible to different languages. The database has six tables and uses indexes to link the contents for a quick access to the data. The first three tables maintains the user's

accounts including name, email, and authorization level, last logon, and index user ID in the first tables; encrypted user's passwords which is using the message digest algorithm 5 (MD5) in the second table; and all the course numbers assigned to the users in the third table. The fourth table maintains the experiments' setting including the name, description, and experiment link, camera link, and the experiment ID. The sixth table contains the time slot schedules. The user ID and experiment ID link every row in the sixth table.

### 2.1.4 Remote Smart Vibration Platform (SVP)

Remote Smart Vibration Platform (SVP) is an experiment developed by the Smart Materials and Structures Laboratory (SMSL) at the University of Houston previously [1]. This experiment is also one of the experiments we brought to Qatar for the remote laboratory at Texas A&M University at Qatar (TAMUQ). Recently people have found smart materials are providing new solution for vibration control [18]. The students can study vibration, controls, vibration controls, and smart materials by conducting SVP experiment which uses smart materials to reduce the vibration of the structure [16], [17].

The SVP device, as shown in Fig. 2-6, is assembled by using fabricated and purchased components. The SVP has a two-story flexible steel frame fixed on top of a plexi-glass box. In the plexi-glass box, there are electric circuit boards made to control the experiment. It was designed and built by students in the SMSL at the UH. Other than the flexible steel frame, the SVP has a motor, Shape Memory Alloy (SMA) wires and a purchased magnetic iron clamped on a container of Magneto-Rheological (MR) fluid. The motor with a weight is mounted on the top of the frame and connected to driver from the box on the bottom. When the user controls the current going through the electrical circuit, the speed of the motor can be adjusted. The rotation of the motor leads the

flexible frame to vibrate. Two SMA wires are hung across the frame. When current goes through the wires, the temperature of SMA will increase. At a certain point of arising temperature, SMA will shrink its length to reduce the vibration of the frame. This is called an SMA brace. A red steel tongue is placed downwards into the container of MR fluid. The magnetic iron clamped on the container can generate magnetic field when it is turned on. That increases the viscosity of MR fluid because MR fluid changes from fluid state to semi-fluid state under the magnetic field. This is called MR damper. The SVP device has a schematic diagram show in Fig. 2-7.

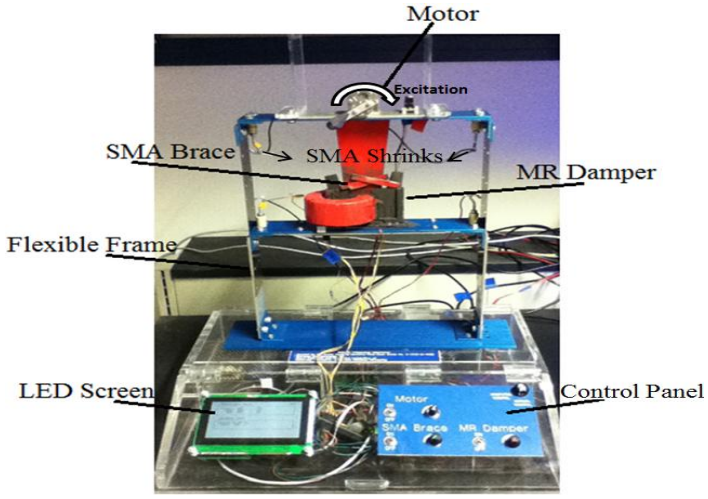


**Figure 2-6:** SVP device

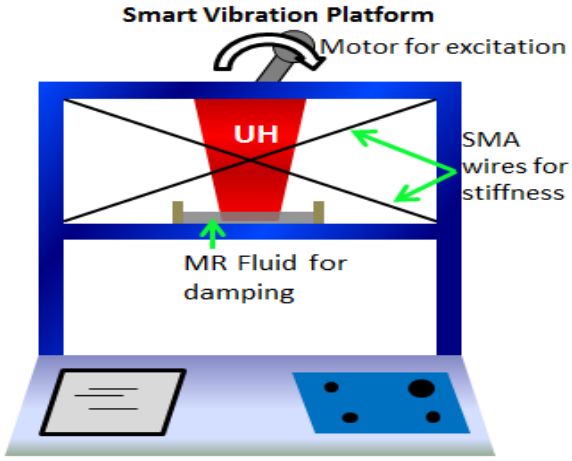


**Figure 2-7:** Schematic diagram of SVP device

The control of the experiment uses LabVIEW VI running in a workstation. The SVP device uses NI data acquisition (DAQ) 6008 USB to sense the feedback from the accelerometers to measure the acceleration, vibration of the platform and temperature of SMA. There are two accelerometers in the SVP device, one at the top of the device next to the motor and the other one under the MR damper. The LabVIEW VI controls the rate of the motor, the power output generated on the SMA wires, and the amount of magnetic field across the MR damper. Fig. 2-8 depicts the VI's front panel for the SVP device. Users can directly change the amplitude of the motor, the SMA brace, and the MR damper in the front panel to control the device. The graph in the front panel plots the two waves for the acceleration at two locations on the frame versa time. A temperature indicator shows the real temperature change on SMA. Users can turn on a filter with a defined cut-off frequency in the front panel to filter away undesired data like noises from the devices and the environment in the lab. The data saving feature works by choosing the time targets in seconds before clicking on the button of recording. An elapsed time block shows the time in seconds after recording.

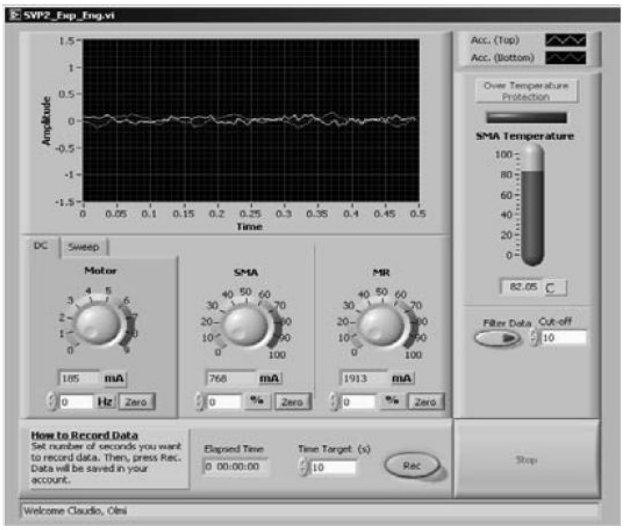


**Figure 2-8:** LabVIEW VI of SVP device (front panel)

## 2.2 Control of Shape Memory Alloy

### 2.2.1 Introduction

Smart memory alloy (SMA) had two phases, Martensite and Austenite. By increasing the temperature, SMA will change from Martensite to Austenite. An SMA wire is easy to be lengthened in the phase of Martensite at the lower temperature and the length will return back to the original length in the phase of Austenite at higher temperature. It is known as the Shape Memory Effect (SME). The force generated by SMA wire in the phase of Austenite is large and the SME is controllable.

SMA has nonlinear response because the hysteresis of SME [26]-[30]. A model of SMA is hard to build [26]. In the theory of nonlinear control, there are several methods we can use, like by using multiple accurate linear equations together to simulate the nonlinear model[35], Bang-Bang and saturation compensator[31], Fuzzy PID controller[30], [34] and sliding mode based robust controller [35], [36],[37]-[40]. Dr. G. Song and Dr. R. Mukherjee have studied the sliding mode based control [24] and Dr. G. Song has successfully built a sliding mode based nonlinear robust controller for a nonlinear system using SMA wire presented in his paper [20]. Our SMA device uses the control method presented in Dr. G. Song's paper.

### 2.2.2 Comparison of Conventional Robust Controllers

In a nonlinear system, the uncertainties of the system are unpredictable or hard to predict in linear equations. The uncertainty in the control of SMA is the hysteresis when SMA returns to its original length. Like many nonlinear system controls, we design nonlinear compensators to control the length change of SMA according to the feedback of the length change of SMA. We will review three conventional robust controllers and

compensators used in nonlinear control, bang-bang compensator, the saturation compensator, and the smooth compensator. In the comparison, we will see the smooth compensator provides more accurate feedback control than other two compensators [31], [32], [33]. That is also the reason why we use the smooth compensator in the control of SMA in our SMA experiment.

Consider the tracking control of SMA and we use the equation from Dr. Gangbing Song's successful implementation of nonlinear robust control on SMA [26]. It uses a smooth compensator to control the displacement of SMA wire. The input is electrical current and the output is the length change of SMA wire. Equations 2.1 to 2.3 are the mathematical model of the compensator,

$$e = y - y^d, \tag{2.1}$$

$$r = \dot{e} + \beta e, \text{ and} \tag{2.2}$$

$$u = u_f - Kr - \rho tanh(ar). \tag{2.3}$$

The aim of the control system is to control the displacement of SMA length. y is the feedback of the system which is the real position of the SMA and $y^d$ is the desired position defined by the users. e is the error between the real position and the desired position. $\dot{e}$ is the derivative of the position error. $u_f$ is a feedforward term to compensate the heat losses and provide a voltage to heat up the SMA [27]. K and r expressed in Equation 2.2 are proportional plus derivative (PD) term and $\rho tanh(ar)$ is smooth robust compensator [26]. The PD term in the feedback control increases the damping to reach the stable state of the system. The smooth robust compensator compensates the hysteresis of SMA, uncertainties in the system and disturbances from the environment. u is the

electrical current or the voltage applied to SMA to control the length change of it. $\beta$, $\rho$, and $a$ are constant tuned in the experiment.

The feedback controller with the bang-bang compensator has expressions shown in Equation 2.4, where the feedforward term and the PD term are the same as that in smooth compensator; and the difference is the bang-bang robust compensator, $\rho sign(r)$ defined by Equation 2.5,

$$u = u_f - Kr - \rho sign(r) \text{ and} \tag{2.4}$$

$$sign(r) \triangleq \begin{cases} 1, & \text{if r} > 0 \\ -1, & \text{if r} < 0 \end{cases}. \tag{2.5}$$

In the bang-bang compensator, when r is larger than zero, the gain of $sign(r)$ is positive one; when r is less than zero, the gain of $sign(r)$ is negative one. The r term defined in Equation 2.2 is dependent on the position error and the derivative of the position error.

The feedback controller with the saturation compensator has expression shown in Equation 2.4, where the difference comparing to Equation 2.4 is the saturation term, $\rho sat(\frac{r}{\varphi})$, defined by Equation 2.5,

$$u = u_f - Kr - \rho sat(\tfrac{r}{\varphi}) \text{ and} \tag{2.4}$$

$$sat(\tfrac{r}{\varphi}) \triangleq \begin{cases} 1, & \text{if r} > \varphi \\ -1, & \text{if r} < -\varphi \\ \frac{r}{\varphi}, & \text{if } |r| < \varphi \end{cases}. \tag{2.5}$$

In the saturation compensator, r is defined by Equation 2.2, and $\varphi$ is constant defined by the user. The saturation compensator has a mathematical expression shown in Equation 2.5: when the variable r is larger than the defined constant $\varphi$, the gain of the

saturation is positive one; when the variable r is less than the negative constant $\varphi$, the gain of the saturation is negative one; and when the absolute value of the variable r is less than the constant $\varphi$, the saturation equals to the value of r divided by the constant $\varphi$, which is $\frac{r}{\varphi}$.

Figure 2-9 shows the chattering results of imperfect control switch and Figure 2-10 shows the three compensators. The bang-bang compensator has an instant change in the magnitude from negative one to positive one; however, the saturation compensator has a linear increase in the magnitude change from negative one to positive one. The smooth compensator has more accurate results comparing to the bang-bang compensator and saturation compensator. The smooth compensator follows the function, $\tanh(ar)$, in the change from negative one to positive one. We can design and tune the value of a in Equation 2.3 and the value of β in Equation 2.2 to affect the shape of the smooth compensator shown in Figure 2-10 (c) till we find a controller with good performance.

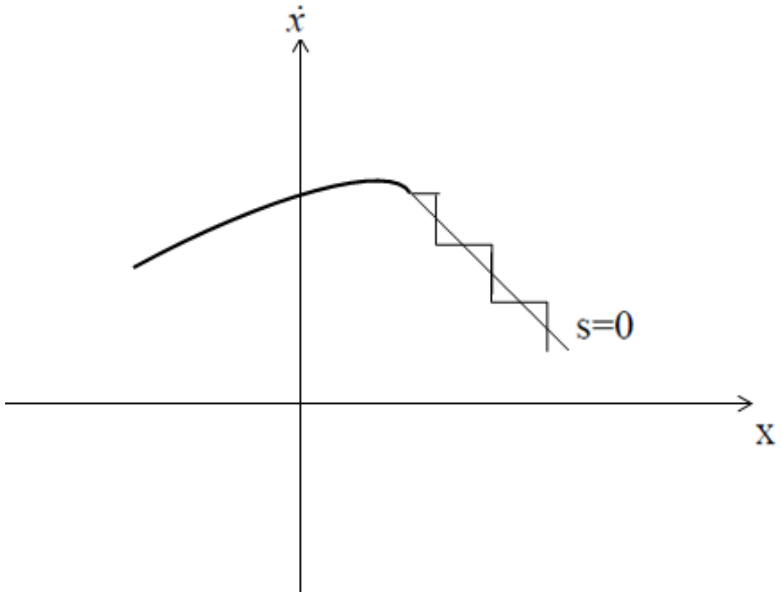


**Figure 2-9:** Chattering as a result of imperfect control switching

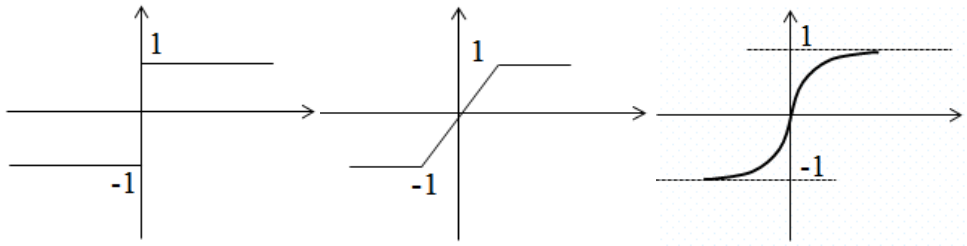


(a) (b) (c)

**Figure 2-10:** Comparison of three compensators: (a) the bang-bang compensator, (b) the saturation compensator, and (c) the smooth compensator

In the comparison of three compensators in Figure 2-10, the smooth compensator in Figure 2-10 (c) provides more accurate control. Thus, we use the smooth compensator in our SMA actuator in SMA device.

# Chapter 3 Shape Memory Alloys and Magneto-Rheological (MR) Fluids

## 3.1 Introduction

Smart materials also called intelligent materials or adaptive materials designed to transform one type of energy into another type to benefit the purposes [41]. For examples, Shape Memory Alloys (SMA) will convert thermal energy into mechanical energy by the length change and shape change of SMA. Piezoceramics materials can convert electric field into mechanical force. They can serve as both actuators and sensors depending on the needs of the users.

## 3.2 Shape Memory Alloys

SMA is a smart material with the ability to return to its original shape. The shape is fabricated during the process of passing the transition temperature band. SMA is durable, electrical conductive, and corrosion resistant.

SMA has a wide application in mechanical engineering, civil structure and medical fields. In the recent study [43] in 2011, factors affecting SMA in retrofit of Islamic minarets has been researched. Application of SMA in civil is not a new topic. In the [44], the results of the application of SMA prestressing devices tested in an aqueduct built on a mountain in 1747 had been presented in 2008. According to the results, the mountain has been protected during earthquake by using the SMA prestressing devices. There are other applications of SMA in our daily life too. For an example, in 2013 Chevrolet C7 Corvette model, SMA has been used to close the pressure vents in the rear hatch of the car, which was advertised as the first application of SMA in the automotive by Chevrolet. For another example, rice cooker must be a device familiar to most people. Actually a rice

cooker uses a SMA spring in combination with another bias spring to control the steam valve. When the temperature is low, the bias spring pulls down the SMA and locks the steam valve. When the temperature is high, the SMA shrinks and pulls up the bias spring to open the valve to let the steam to exit. In the following, we will have a general review on the important properties of SMA.

### 3.2.1 Shape Memory Effects

A typical SMA wire has low yield strength when the temperature of SMA is below the transformation temperature of it. As a result, the SMA wire can have deformations like elongation and twists by applying little force to it. Because of the property of SMA, when the temperature of SMA is increased to be higher than its transition temperature, the SMA wire can return to its original shape and a large force is produced during the process of shape recovery. This is called shape memory effects (SME) that the alloy remembers its original shape.

SME is caused by the atomic change in crystal structure of the material. SMA has two phases Austenite at high temperature and Martensite at cool temperature. When the temperature is high, the crystal structure of the alloy is at austenite phase where the orientation of atoms is cubic and the structure is very strong. After cooling SMA, the temperature decreases below transformation temperature. The atomic crystal structure of the alloy at Martensite becomes twinned monoclinic before any deformation. When the alloy at Martensite is being deformed by applied force, the atomic crystal structure becomes detwinned. This is called one-way SME as shown in Figure 3-1 [42]. There is another type called two-way SME. The alloy of two-way SME will return to one of its original shapes like one-way SME at heating process. What make two-way SME two-

way is that the alloy with two-way SME has two shapes memorized. At cooling process, it will recover to a low temperature shape. Additionally, the recovery at cooling temperature could only generate a little force which is just large enough to recover the shape. It would affect nothing on the external mechanical parts.

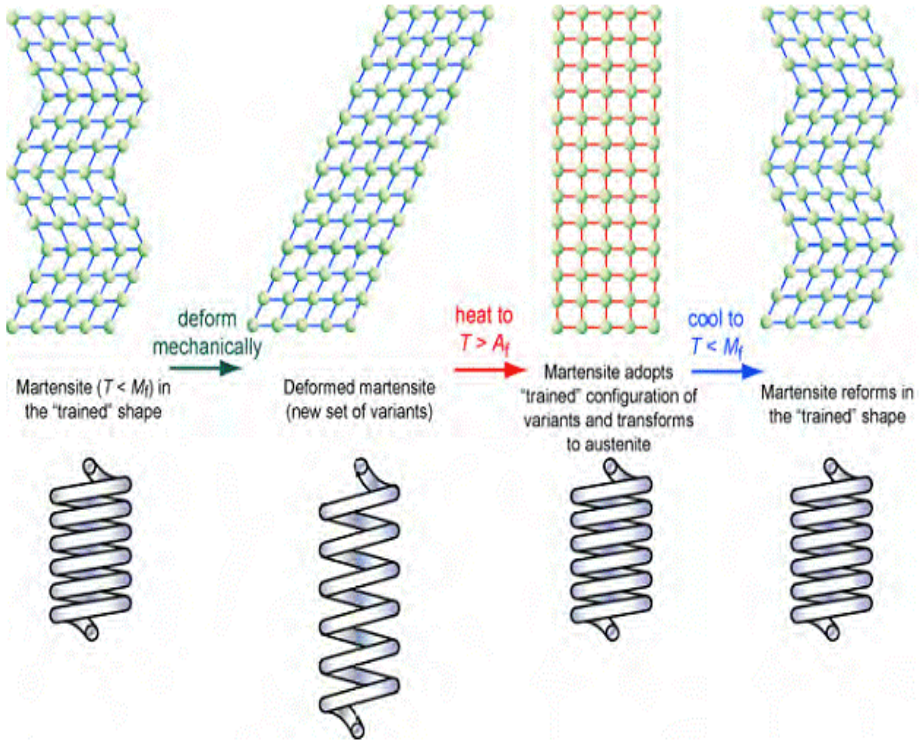


**Figure 3-1:** Microstructural change of the shape memory effect

### 3.2.2 Hysteresis of Shape Memory Alloys

In the phase transformation of SMA, the property of hysteresis of SMA is observed. It means that the loop of heating and cooling does not overlap. For example, an SMA wire is elongated by a constant force. When the temperature of the SMA wire is being increased by the heat, the SMA wire shrinks back to its original length even though the force is still there. When the heating source is gone, the temperature of SMA is starting to decrease. The phase of SMA changes from Austenite at higher temperature to Martensite at lower temperature. The SMA wire at Martensite is elongated by the force again. The

phase change of Martensite and Austenite has different starting temperatures and finishing temperatures. The temperature of Austenite is always higher than the temperature of Martensitre. The finishing temperature of Austenite is larger than the starting temperature of Austenite. The starting temperature of Martensite is always larger than the finishing temperature of Martensite. The phase transformation for the SMA wire actuator is shown in the diagram displayed in Figure 3-2 [41]. The gap between Martensite line and Austenite line is the transformation hysteresis.

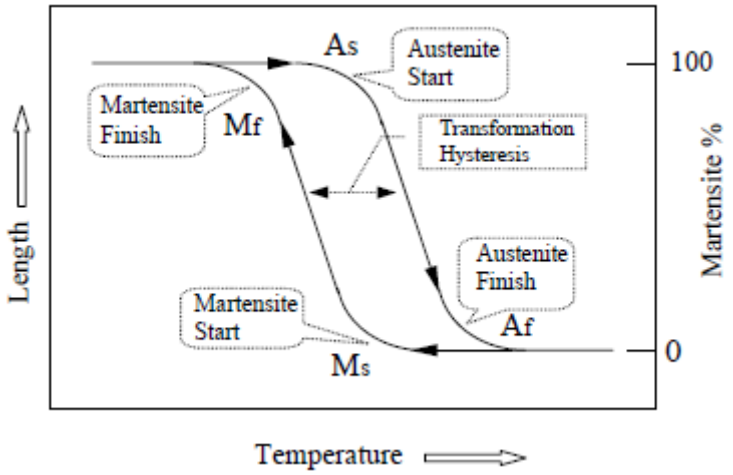


**Figure 3-2:** Hysteresis of phase transformation

## 3.3 General Review of Magneto-Rheological Fluids

Magneto-Rheological (MR) is field-dependent materials. MR is suspensions of micron-sized and magnetizable particles in oil. MR fluids have viscosity change in response to magnetic fields. The application of them is most likely shock absorbers used in various dampers in cars, buildings and airplanes etc.

MR fluid changes its viscosity under the presence of magnetic fields. Under regular condition without the presence of magnetic fields, it is in fluid state and free to flow; however, with the presence of magnetic fields, it transforms to semi solid state and the

viscosity increase. The atoms arrangement of MR fluid aligns in the direction of the magnetic field. The change happens in milliseconds and it is reversible.

As the increase of the magnetic flux across the MR fluid, the strength of the resistance to the movement in MR fluid increases. In other words, the viscosity and the strength are controllable by controlling the magnitude of the magnetic field. Many applications like dampers use such property to design semi-smart dampers to control the damping of the system based on the change of the external environment by adjusting the magnitude of the magnetic field across MR fluid. The increase of viscosity decreases the damping of the system.

MR fluids have several advantages comparing to ER fluids according to the class note in Intelligent Structural System, 2013[41]. ER fluids are like MR fluids, but the difference is that ER fluids use electrical field to activate the transformation of the fluids unlike the MR fluids use magnetic field. Firstly, MR fluid has higher max yield. Secondly, the running power of two fluids is both from 2 to 50 watts; however, the working voltage of ER fluids is from 2 to 5 kV which is much larger than the working voltage of MR fluids from 2 to 25 V. Low working voltage provides many advantages such as safe and convenient to use at regular power supplies. Thirdly, MR fluids are very stable and unaffected by most impurities unlike ER fluids cannot tolerate impurities.

MR fluids follow the models show in Figure 3-3 [41]. The graph has strain rate as the x-axis and shear rate as the y-axis. The straight linear line is the Newtonian fluid behavior line. MR fluids follow Newtonian line in the absence of magnetic field. Usually controllable fluids follow the Bingham model in the absence of applied field [45]. The Bingham model has three parts: an increasing linear line with negative magnitude when

the strain rate is less than zero; an instant increase of the shear stress when the strain rate is zero; and another increasing linear line with positive magnitude when the strain rate is larger than zero.

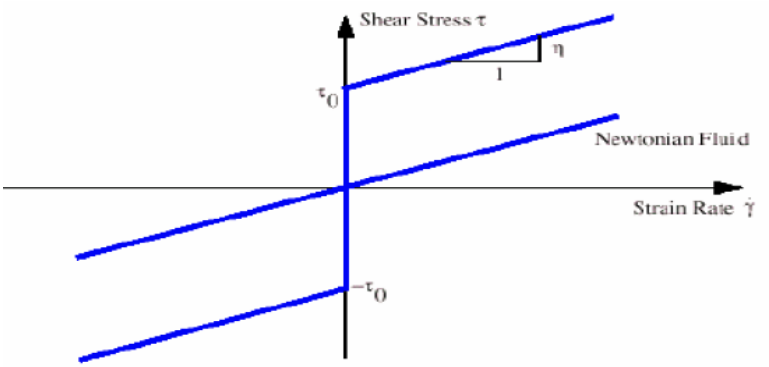


**Figure 3-3:** Bingham model of controllable MR fluids

Equation 3.1 presents the Bingham Model and Equation 3.2 presents the behavior of Newtonian fluids,

$$\tau = \tau_0(H) + \eta\dot{\gamma} \text{ and} \tag{3.1}$$

$$\tau = G\gamma. \tag{3.2}$$

In Equation 3.1, τ is the fluid stress, $\tau_0$ is the field dependent yield stress, $\eta$ is the plastic viscosity (i.e., at H=0), and $\dot{\gamma}$ is the strain rate. It describes the fluid stress τ larger the field dependent yield stress $\tau_0$. In Equation 3.2, τ is the fluid stress, G is the complex material modulus, and γ is the strain. It describes the fluid stress τ less than the field dependent yield stress $\tau_0$. The complex material modulus G is also field dependent [46], [47].

In the real MR fluids, their behavior has difference comparing to the prediction made by Bingham model. Non-Newtonian behavior of MR fluids in the absence of magnetic field is most likely the cause of the difference in the real MR fluids [48]; however, Bingham model is still good to use in many designs.

The shear stress of MR fluids is depending on the strength of the applied magnetic field. MR fluids have larger shear stress when the strength of the applied magnetic field is larger. The increase of shear strain rate increases the magnitude of shear stress, but not a significant change. Figure 3-4 [41] depicts the shear stress change with the shear strain rate change at different magnetic field in regular MR fluids at the temperature of 25°C.

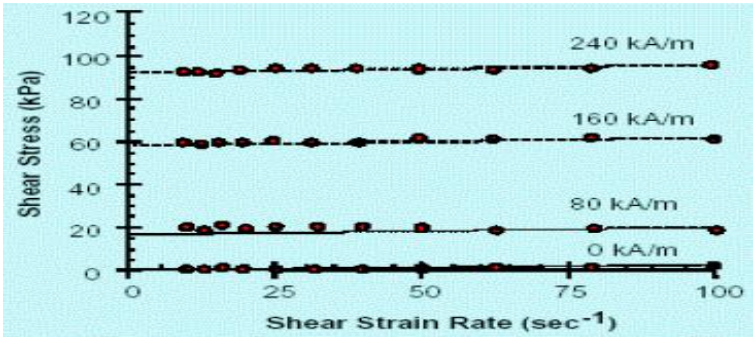


**Figure 3-4:** Shear stress change with the shear strain rate change in different applied magnetic field across MR fluids at 25°C

Magnetic induction, B, describes the magnetic flux density in MR fluids at 25°C. Figure 3-5 [41] depicts the magnetic induction change vs. the magnetic field change. As we can see in Figure 3-5, the red line shows that the magnetic induction in MR fluids increases at a high rate, but the increase rate slows down after, because MR fluids have upper/lower limit to magnetic flux density which may be achieved.

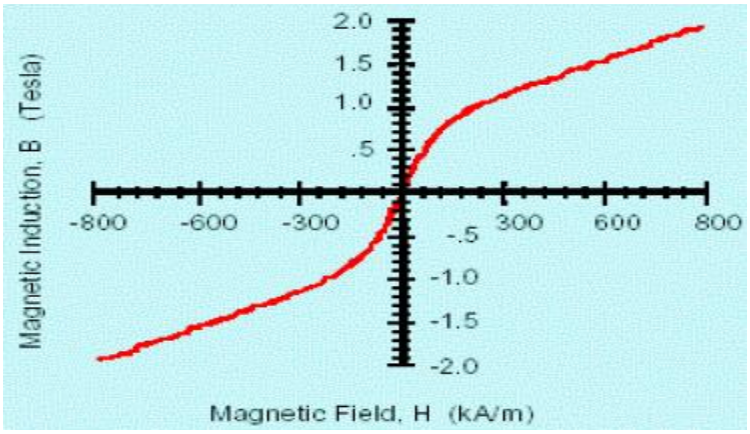


**Figure 3-5:** "B – H" curve of regular MR fluids at 25°C

## 3.4 Summary

Smart materials are intelligent materials or adaptive materials designed to transform one type of energy into another type to benefit particular purposes. They have four classes, field-dependent materials, shape-memory materials, smart glasses and others. SMA is shape memory materials. It has SME which enables SMA to return to its original shape after deformation by heating SMA up. MR fluids are field dependent materials. In the presence of magnetic field, MR fluids change from liquid state to semi solid state with the increase of viscosity, which follows Bingham model. In our remote laboratory with two remote experiments using SVP device and SMA device, we use these two smart materials SMA and MR fluids to allow the students to study the vibration and vibration control, and the hysteresis of SMA.

# Chapter 4 Shape Memory Alloys Experiment

## 4.1 Introduction

The Shape Memory Alloy (SMA) experiment is developed to demonstrate and analyze the characteristics of SMA. It is used to study the hysteresis behavior of the wire actuator (SMA) and how the driving frequency changes the hysteresis loop. The experiment can apply sinusoidal driving signals (AC) of 16.4 Volts in magnitude and respectively from 1/30Hz to 1/50Hz in frequency to the SMA actuator. Students can observe the wire movement through the webcam in the remote laboratory. They can record a number of cycles such as five for each test. Saved data are applied voltage, displacements of the wire actuator, and time in seconds. The data will be used for future analysis.

The SMA experiment includes two parts, experimental hardware equipment setup and experimental software development in workstation. The experiment consists of an SMA wire actuator connected to the electronic circuitry that controls the current going through SMA wire to heat it up. Once the SMA actuator is heated up to transition temperature, the length will start to decrease due to shape memory effects (SME). A linear sensor is attached to the SMA actuator to sense the displacement change. The displacement change caused by the temperature change in SMA will be recorded through the sensing device National Instruments (NI) DAQ 6008 which is connected to a workstation. NI Laboratory Virtual Instrument Engineering Workbench (LabVIEW) is installed in the workstation and programmed Virtual Instrument (VI) is running to control the experiment.

## 4.2 Experimental Setup

The experiment consists of a web camera, a workstation, and NI Data Acquisition (DAQ) 6008 USB, a DC power supply, and the SMA device, as shown in Figure 4-2. A PC workstation, as shown in Figure 4-1, runs LabVIEW to control the voltage applied on the SMA wire actuator. NI DAQ 6008 USB is a hardware device talking to the experiment and the PC. It generates voltage output based on the signal from LabVIEW and senses the voltage changes in the experiment to control the amount of voltage on SMA wire. The DC power supply, generates constant voltage applied on SMA. Pulse-width Modulation (PWM) is the method we used to control the voltage from the DC power supply with the implementation of a Solid State Relay (SSR). SSR can switch the circuitry connected to the DC power supply in series on and off swiftly to achieve an effect that a constant value of voltage is applied on the SMA wire. To have a real-time experiment, the camera is used to view the experiment remotely. By applying voltage on SMA wire, the temperature of SMA will increase and the length of the wire will decrease.

The SMA device is assembled by using both fabricated and off-the-shelf components. The main frame uses L shape aluminum bar fixed by screws. There are plexi-glass sheets fixed on several sides of the SMA to protect and decorate the experiment. On the bottom, blue LED lights are used to light up the experiment. In the middle of SMA device, a red painted block is lifted by SMA wire actuator and pulled down by two springs at the same time. When the force generated by the SMA is larger than the force generated by two springs, the direction of the force in summation is pointing towards up and the block will be lifted up by SMA. A linear powered sensor is used to measure the displacement of the block. Output data in voltage from the displacement sensor is collected by DAQ 6008

and converted into displacement by programmed algorithm in the VI loaded in the workstation.

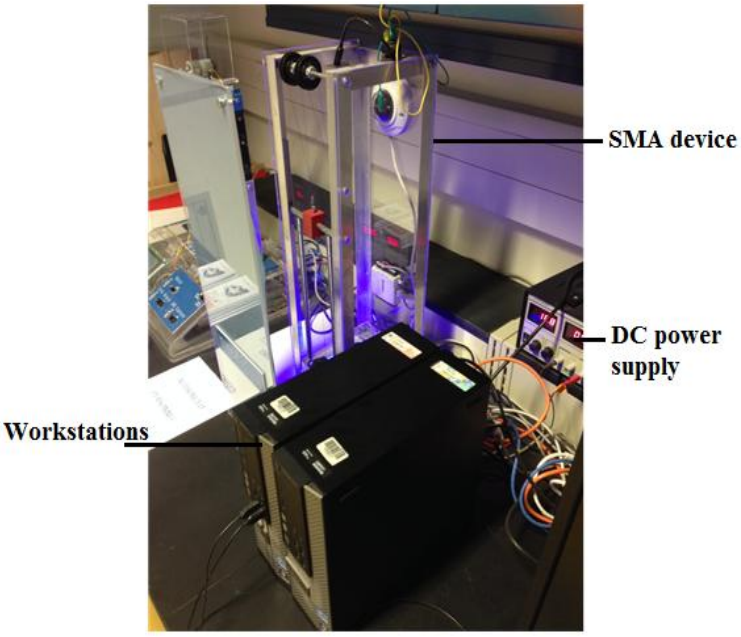


**Figure 4-1:** SMA device, workstations, and DC power supply

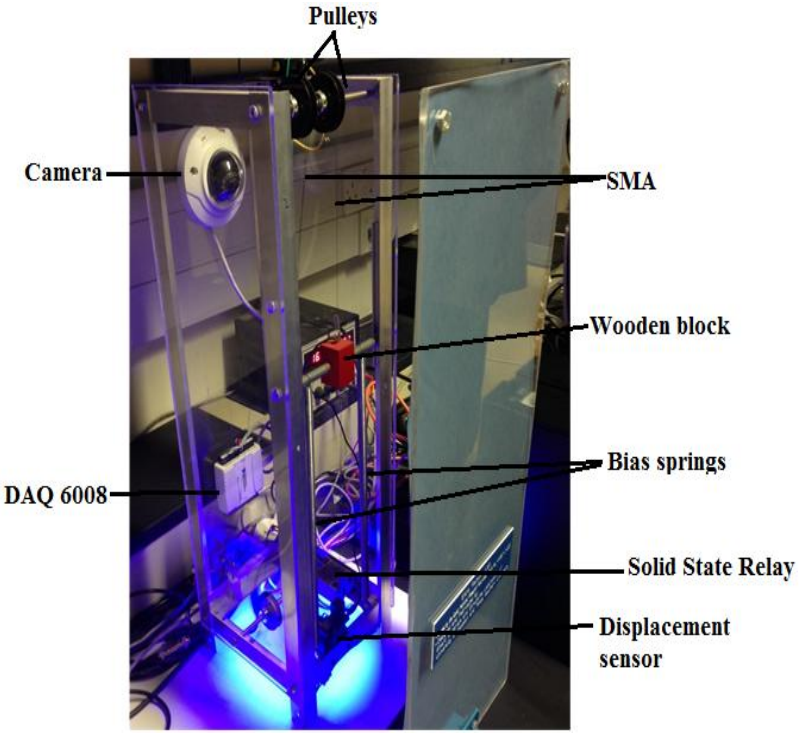


**Figure 4-2:** SMA device

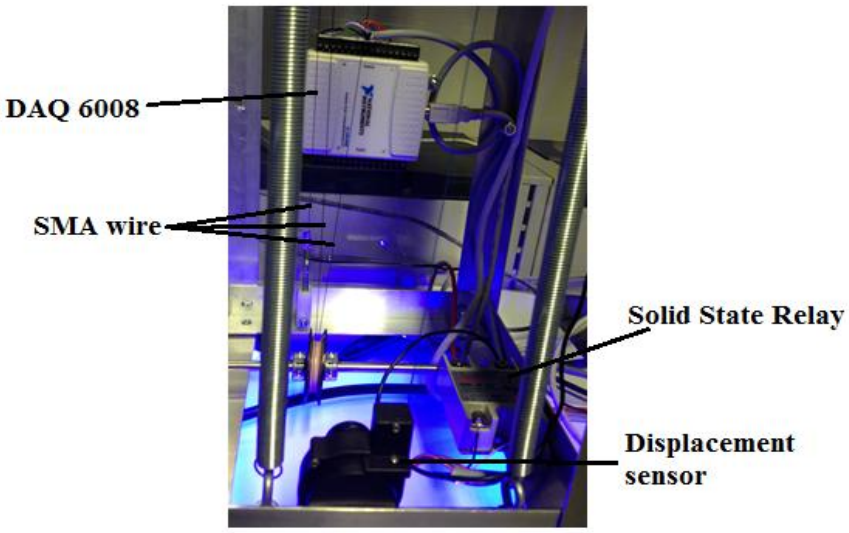


**Figure 4-3:** DAQ 6008, displacement sensor, and Solid State Relay (SSR)

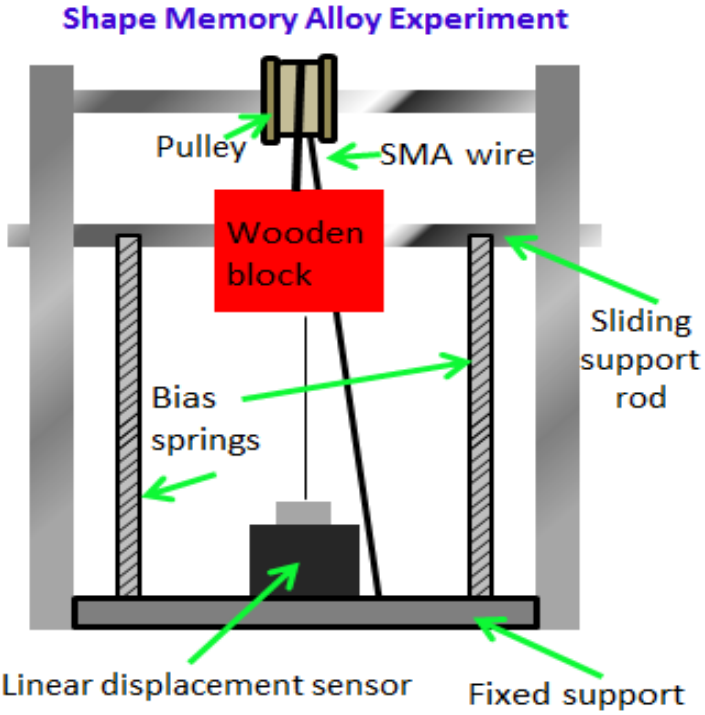


**Figure 4-4**: Schematic diagram of SMA device

## 4.3 Control of the Shape Memory Alloy Experiment

In the experiment, there are two parameters need to be controlled, one is the displacement of the block and the other one is the desired value of voltage applied on

SMA wire. The voltage applied on SMA is controlled using Pulse Width Modulation (PWM) and the displacement of the block can be controlled using a sliding mode based controller [26]. PWM has benefits of generating signals with ease to change its frequency, voltage magnitudes and forms [50]. It compares with a carrier signals and the desired signals to switch the circuitry connected with the DC power supply in series on and off to achieve the same effects as the desired signals in an efficient and flexible way. In the displacement control of SMA, we are facing one difficulty that the response of SMA is nonlinear due to the hysteresis of SMA [28]. Based on the successful research done before, a sliding mode based controller is well competitive with other nonlinear controllers, like bang-bang control for our purpose [26], [49]. The algorithm of PWM and a sliding mode based controller are programmed and implemented in LabVIEW VI. The data of the real displacement of SMA is collected by NI DAQ 6008. The programmed VI reads the real displacement and then the controller module in VI computes desired voltages before the PWM module in VI. Controlled signals are then output from the VI through DAQ 6008 to the connected circuitry to achieve the displacement control of SMA.

### 4.3.1 A Sliding Mode Based Controller for Displacement Control

In the task of controlling the displacement, the system was nonlinear due to the hysteresis of SMA [28]. As we discussed in Chapter 2, a sliding mode based controller was designed based on the successful controller of an SMA wire actuated flap presented in paper [26]. Based on Equation 2.1 to 2.3, the controller is shown in the following,

$$V = V_f - Kr - \rho \tanh(ar). \tag{4.1}$$

After tuning in the experiment, Eqn. 2.2 and Eqn. 4.1 become,

$$r = \dot{e} + 15e \text{ and} \tag{4.2}$$

$$V = 10 - 15r - 1\,tanh(-1r), \tag{4.3}$$

where V is the output voltage.

### 4.3.2 Pulse Width Modulation

PWM has benefits of generating signals with ease to change its frequency, voltage magnitudes and forms to control the output applied on the experiment [51], [52], [53]. By comparing a carrier signal, c (t), to a reference signal, r (t) as shown in Figure 4-5, it generates a constant-frequency (CF) PWM signal. In CF PWM, there are three types of carrier signals commonly used, sawtooth carrier (Figure 4-5b), inverted sawtooth carrier (Figure 4-5c), and triangle carrier (Figure 4-5d). In our experiment, we will use CF PWM because we are using signals of constant frequency for the voltage output applied on the SMA actuator.

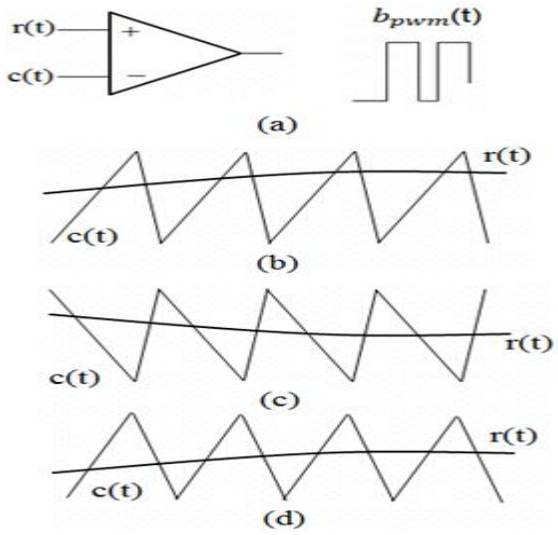


**Figure 4-5:** Constant frequency PWM implemented by a comparator with different carrier signals

The reference signals have leading edge and trailing edge. In sawtooth carrier, the leading edge is rising instantly and the trailing edge (falling) is modulated as the

reference signal level changes, which is referred as constant-frequency trailing-edge modulation. In inverted sawtooth carrier, the trailing is falling instantly and the leading edge (rising) is modulated as the reference signal level changes, which is referred as constant-frequency leading-edge modulation. In triangle carrier, the leading edge and the trailing edge are both modulated. Two edges are symmetric to ensure the pulse is place in the middle of a carrier cycle when the reference signal is a constant. It is referred as constant-frequency double-edge modulation.

Trailing-edge modulation is used most like in DC-DC conversions and double-edge modulation is commonly used in AD-DC and DC-AC conversions, because double-edge modulation can reduce the effects from some harmonics in sinusoidal signals [50]. There are two sets of PWM signals generated separately with either of the reference signals of trailing-edge modulation and double-edge modulation, as depicted in Figure 4-6 and Figure 4-7 [50]. As we can see from two figures, the reference signals, r (t), is comparing with the carrier signal, c (t). When the amplitude of the reference signal is larger than the amplitude of the carrier signal at time t, the PWM signal, $b_{pwm}$, has a step value at the same time instant. Similarly, when the amplitude of the reference signal is smaller than the carrier signal, the PWM signal has a value of zero.

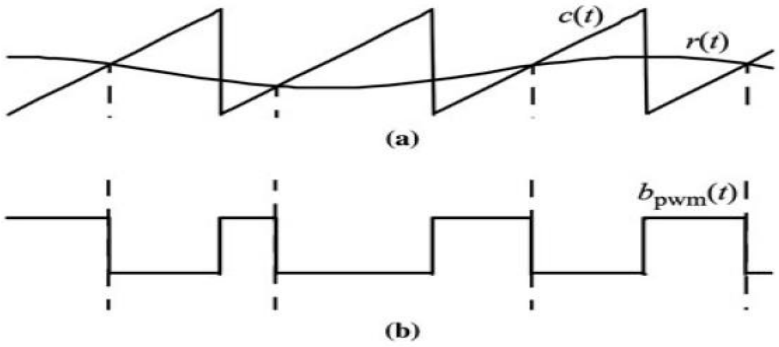


**Figure 4-6:** Trailing-edge modulation

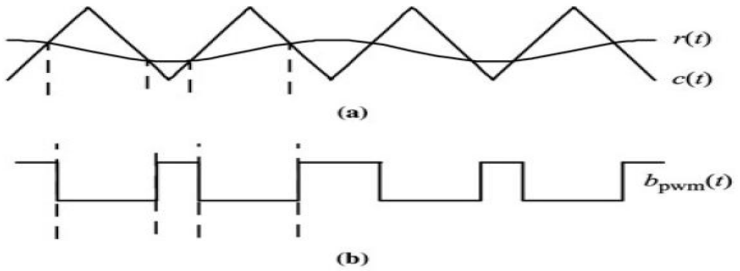


**Figure 4-7:** Double-edge modulation

In the experiment, we used double-edge modulation instead of trailing-edge modulation. The carrier signal in the SMA experiment is a sinusoidal wave with frequencies from 1/30Hz to 1/50Hz. The frequency of the carrier signal is adjustable by the client. The parameters of the reference signal of SMA experiment are tuned in the real experiment to ensure the best outcome of the performance.

## 4.4 LabVIEW Algorithm

The SMA experiment is implemented and run by programed VI of LabVIEW in the workstation. The VI has several parts as we have mentioned in previous chapters, such as sliding mode control codes, and PWM codes. In this section, we will discuss more about the implementations of sliding mode based controller and PWM in LabVIEW.

### 4.4.1 Implementation of Sliding Mode Based Controller in LabVIEW

The displacement control in the SMA experiment is using a sliding mode based controller. As shown in Figure 4-5, the control has two parts, measurement of the displacement and computation of the real-time control. The measurement of the displacement is performed by an electrically powered linear sensor. The sensor generates voltage output as response to the displacement of the SMA wire in a mathematically linear relation. The conversion from the voltage measurement to the displacement

measurement is implemented using LabVIEW. In the Figure 4-9, we have the LabVIEW code of showing how the conversion from the measured displacement in voltage to the displacement in inch is implemented in the real experiment. The relation can also be expressed in the following equation,

$$\mathrm{D(in)} = \frac{\mathrm{D(volts)} - 2.048}{4.63 \times 0.039318}, \tag{1}$$

where 2.048 is a tuned constant for the real experiment, 4.63 is the driving voltage of the linear sensor, and 0.039318 is a constant predetermined by the manufacturer of the linear sensor used for the conversion from voltage measurement to displacement measurement.

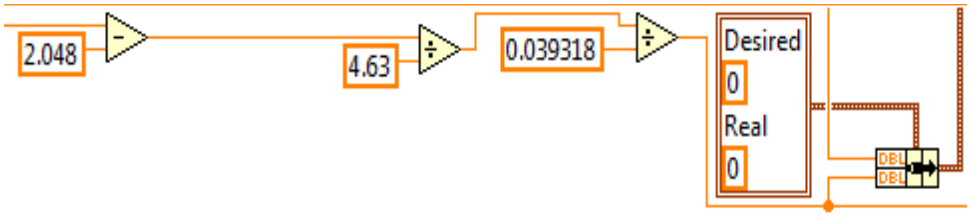


**Figure 4-8:** Displacement measurement code in LabVIEW

The sliding mode based controller expressed in Equation 2.1, 2.2, and 4.3 are implemented in LabVIEW as shown in Figure 4-10. The parameters of the sliding mode based controller are tuned in the experiment. New form of the equation is expressed in the following,

$$V = V_f - Kr - \rho \tanh(ar). \tag{4.1}$$

After tuning in the experiment, Eqn. 2.2 and Eqn. 4.1 become,

$$r = \dot{e} + 15e \text{ and} \tag{4.2}$$

$$V = 10 - 15r - 1 \tanh(-1r), \tag{4.3}$$

where V is the output voltage in Equation 4.1 and Equation 4.3.

In LabVIEW, the error in Equation 2.1 can be calculated by letting the desired value of displacement subtract the value of the measured displacement. The control variable of

r is expressed in the terms of the variable of error and the variable of the derivative of error. The derivative of error is calculated by dividing the error of displacement by the time difference between each data measurement. The function of tanh is provided in LabVIEW that we can directly use it. The feedforward constant $V_f$ is tuned to be 10 volts to compensate the heat loss in the environment. Other constant of the controller are tuned based on the performance of the SMA experiment. It has a disadvantage that if any big the environmental change or external change occurred to the SMA experiment, the parameters in the controller would need slight modifications to achieve the best performance in the SMA experiment.

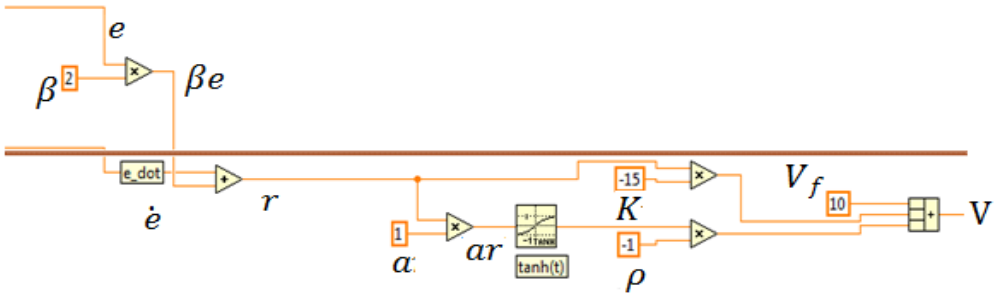


**Figure 4-9:** Implementation of sliding mode based controller in LabVIEW

### 4.4.2 Implementation of Pulse Width Modulation in LabVIEW

In the implementation of PWM, we have two signals, carrier signal and reference signal, to be compared. We use an express VI from LabVIEW to simulate a triangle signal as our reference signal. The configuration of the reference signal for the SMA experiment is 12.5Hz in frequency, 3.5 in amplitude, and 8 for offset. There are 50 samples per second and five samples are generated per loop. In other words, every triangle in the reference signal needs 100miliseconds to be generated. The carrier signal is generated by using the same express VI as used for the reference signal with the signal type to be DC rather than triangle. The configuration of the DC signal is eight for offset,

and the simulate acquisition rate is 50 samples per second and 5 samples per loop, which is the same as the simulate acquisition rate for the triangle signal. The same simulate acquisition rate between the reference signal and the carrier signal makes two signals comparable in calculation. In the comparison of two signals, once the amplitude of the carrier signal is larger than the amplitude of the reference signal, the value of pulse is positive. In the implementation of such a comparison in LabVIEW, we subtract the reference signal from the carrier signal and compare the value after subtraction to zero. If the value is negative or less than zero, the Boolean VI of less and equal to zero returns true to the case structure, otherwise, it returns false to the case structure. The return from the case structure is zero when it is true and one when it is false. The value is amplified by five and returns to the VI of data output. Repeating of the algorithm will create the PWM signal.

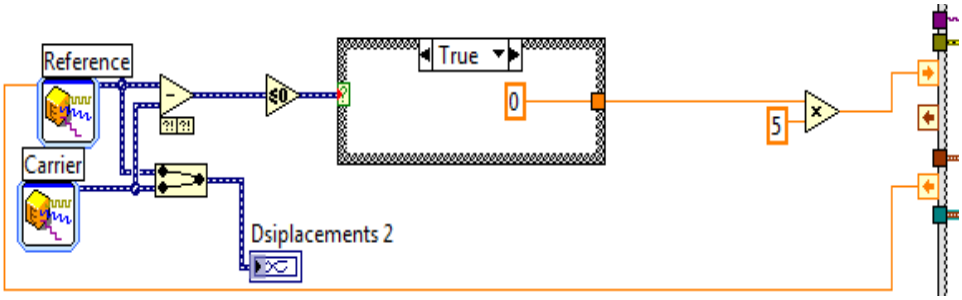


**Figure 4-10:** Implementation of PWM in LabVIEW

## 4.5 Shape Memory Alloy Experiment Results

The purpose of the SMA experiment is to study the hysteresis of SMA affected by the driving frequency and the feedback control of SMA. The SMA is driven at various frequencies to demonstrate the hysteresis change. The feedback control of the displacement is demonstrated by using square wave and sinusoidal wave with different amplitudes.

### 4.5.1 Hysteresis of Shape Memory Alloy in Experiment

We conducted the SMA experiment at three different frequencies, 1/20Hz, 1/30Hz, and 1/50Hz. The driving signal type was sinusoidal signal for all three signals. The amplitude of the voltage applied on the SMA actuator was 16.7 volts which was consistent in the experiment. The displacement of the SMA at three frequencies vs. time in second is plotted in Figure 4-11. A driving signal with smaller frequency provided more time to heat the SMA wire. It provided the SMA more time and higher temperature to contract more in length at higher frequencies. That is the reason why we observe that the response at 1/50Hz has larger displacement and longer time per cycle than those of the response at 1/30Hz and the response at 1/30Hz has larger displacement and longer time per cycle than those of the response at 1/30Hz. The displacement was measure by the linear displacement sensor and processed by the VI in LabVIEW. The data of the displacement and the time can be saved to the directory by the saving feature in the VI.

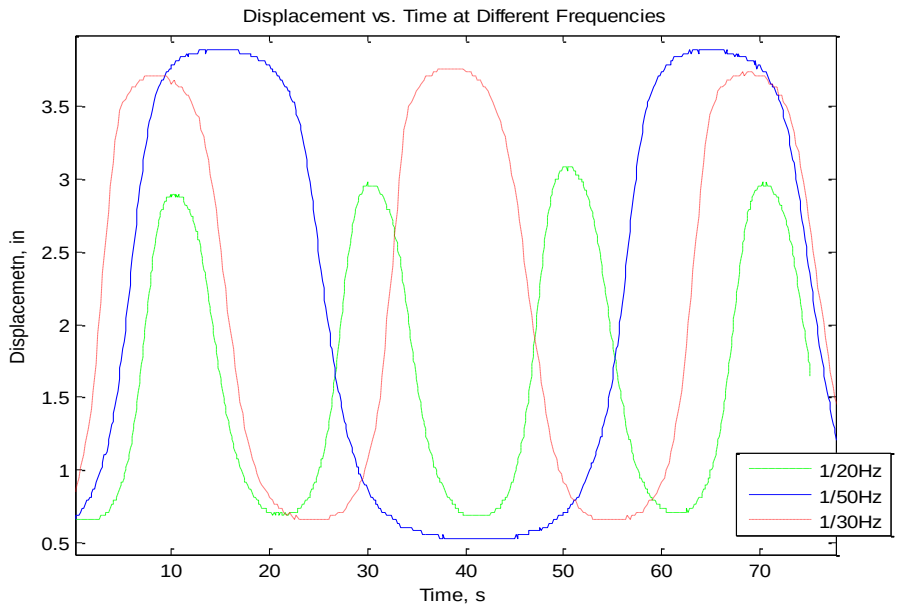


**Figure 4-11:** The displacement vs. time at three frequencies of 1/20Hz, 1/30Hz, and 1/50Hz

Hysteresis was a significant behavior of SMA. SMA wire could dissipate energy through hysteresis. As the temperature increased in the SMA wire, the wire basically changed its phase from Martensite to Austenite. It tended to shrink to its original shape. The change of position of the weight divided by the original length of SMA wire 45'' was the strain. We also observed that the increase of voltage increased the strain of SMA in Figure 4-12, Figure 4-13, and Figure 4-14, because the increase of voltage would eventually increase the temperature in the SMA wire.

Three figures are also showing the hysteresis of SMA at 1/20Hz, 1/30Hz, and 1/50Hz. The hysteresis loop at higher frequency has larger strain than that at the lower frequency. We can see that the shape of hysteresis loop is also affected by the change of frequency of the driving force. The shape change is more obvious if we compare the Figure 4-14 to Figure 4-12/Figure 4-13, because 1/50Hz is much slower than 1/20Hz and 1/30Hz.

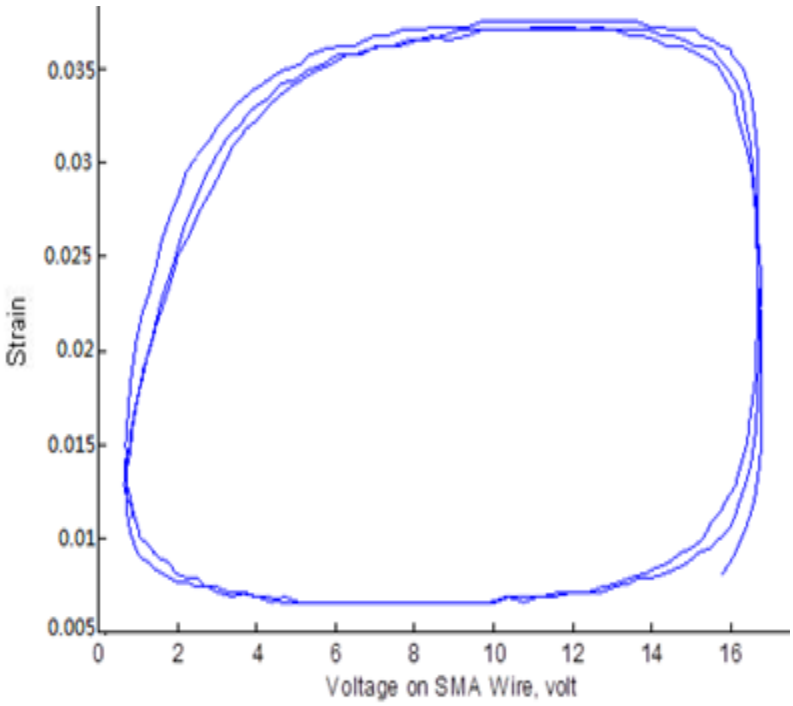


**Figure 4-12:** The hysteresis loop at 1/20Hz

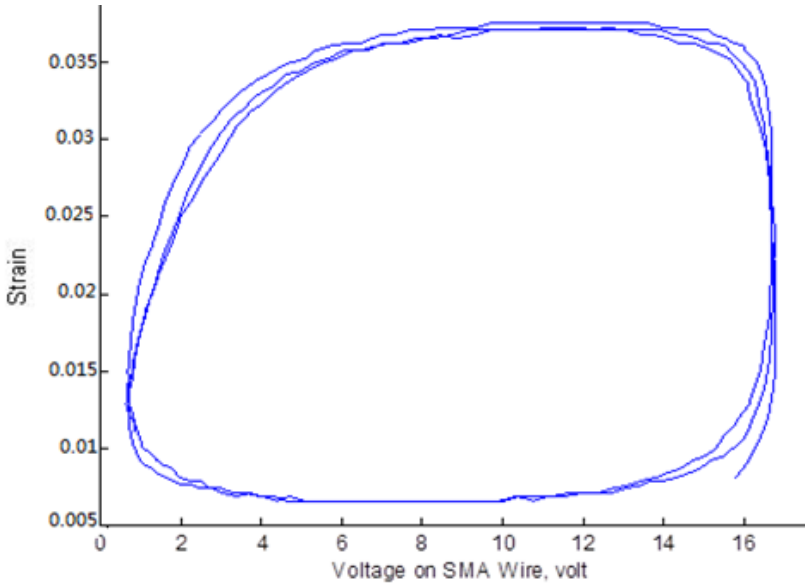


**Figure 4-13:** The hysteresis loop at 1/30Hz

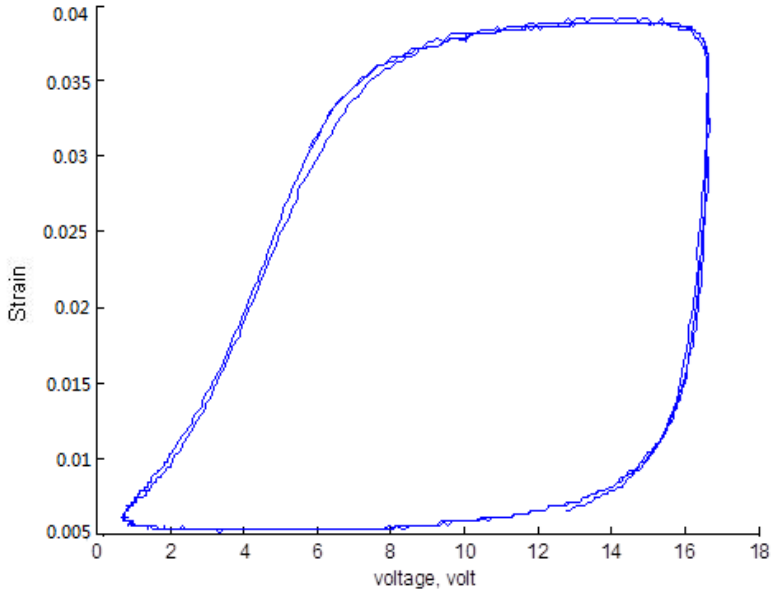


**Figure 4-14:** The hysteresis loop at 1/50Hz

### 4.5.2 Application of Feedback Control of Shape Memory Alloy

In the task of displacement control for the block, we used a sliding mode based controller programmed in LabVIEW. Users were allowed to set the block to move to any position requested. In the following, there are demonstrations of tracking performance using square waveform signals and sinusoid signals programmed in LabVIEW.

We conducted four trials of feedback control of the displacement for the SMA experiment. We used two tracking signals, square wave signal and sinusoidal signal, as our reference (desired displacement) in the control. The results of the control and the error are plotted in Figure 4-15.

The tracking of the displacement is good in general. Including the effect of the hysteresis of SMA wire, the tracking errors are listed in the following. The mean error is 0.65in for square waveform signal with magnitude of 3 and 0.36in for the one with magnitude of two. The mean error is 0.051in for the sinusoid signal at 1/40Hz and 0.063in for the one at 1/30Hz. The hysteresis of SMA wire is the major reason causing the large tracking error in square waveform signal because these signals have sudden drops and rises, however, once the signal is following the sinusoidal signal in a slow frequency, the tracking is smooth and accurate. We can conclude that this feedback control is working well under a slow frequency and a continuous move because SMA wire needs time to react, but it will have a delay in response if the desired displacement has a change in sudden.

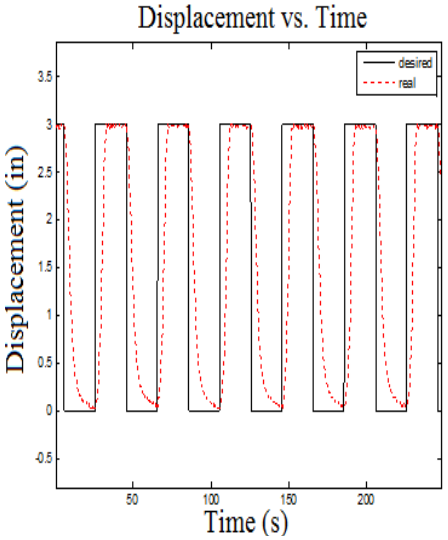

(a)

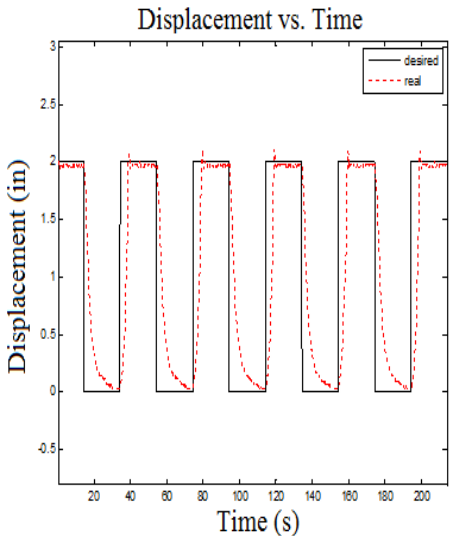

(b)

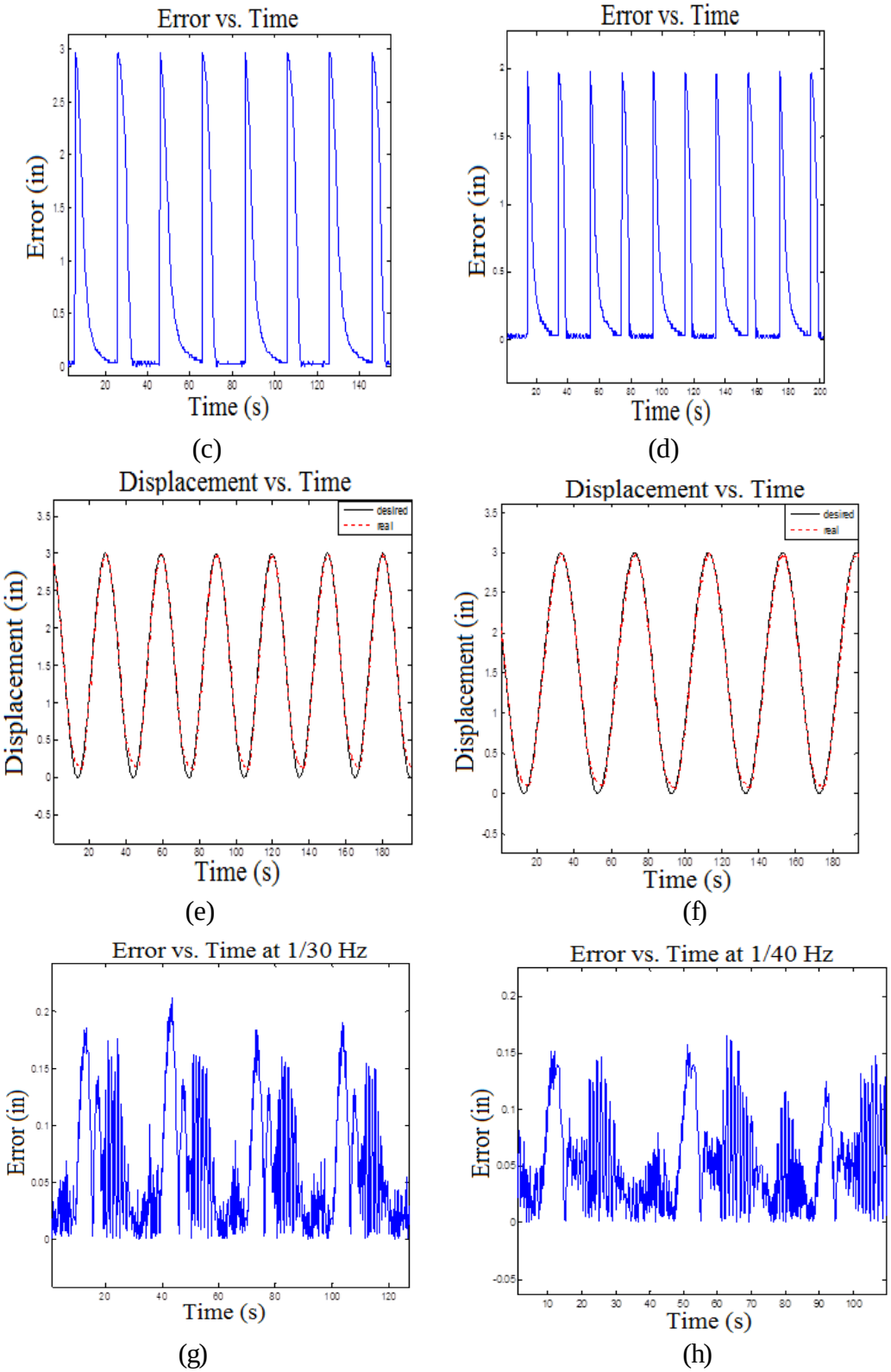


**Figure 4-15:** Tracking performance and performance error

Figure 4-15: (a) tracking performance of square waveform signal of magnitude of three (b) tracking performance of square waveform signal of magnitude of two (c) tracking error of square waveform signal of magnitude of three (d) tracking error of square waveform signal of magnitude of two (e) tracking performance of sinusoid signal at 1/30Hz (f) tracking performance of sinusoid signal at 1/40Hz (g) tracking error of sinusoid signal at 1/30Hz (h) tracking error of sinusoid signal at 1/40Hz.

## 4.6 Summary

The SMA device has been built by students from UH and TAMUQ. The aim of the SMA device is to study the hysteresis of SMA and how the driving frequency changes the hysteresis loop. From the experiment results, we have observed the hysteresis of SMA and the effects of the driving frequency on the hysteresis loop. The SMA device uses NI LabVIEW VI for the control of the experiment. SMA is nonlinear in displacement control due to the hysteresis. Thus, the displacement control of SMA uses sliding mode based controller and smooth robust compensator. We use PWM method to control the applied voltage on SMA by using an SSR to swiftly switch the electric circuitry on/off. We integrate the SMA experiment into the novel remote laboratory at TAMUQ (Chapter 5) for the students to study the experiment remotely.

# Chapter 5 Novel Remote Laboratory

## 5.1 Introduction

Remote laboratory is the use of telecommunications technology to allow remote control physically set up experiments from anywhere in the world. A novel remote laboratory at TAMUQ has been developed through the collaborative effort of Texas A&M University at Qatar (TAMUQ), the UH, and the TSU. The novel remote laboratory with the advantage technology has two parts, the server/experiment part, and server/client part (done by Mr. Ning Wang [56]). The advanced technology uses the LabVIEW to Node.js (LtoN) in the server/experiment part to build a quick, reliable and plug-in free remote laboratory. The experiments are controlled by coded Virtual Instrumentation (VI) in LabVIEW. The client web application (done by Mr. Ning Wang [56]) uses the Web 2.0 Technology including HyperText Markup Language (HTML), Cascading Style Sheets (CSS), and JQuery/JQuery-Mobile JavaScript libraries. The server application is built on MySQL Database, Apache web server engine and Node.js web server engine. Real-time communication among server, web, and experiment uses JSON and Socket.IO communication module.

## 5.2 Remote Laboratory at Texas A&M University at Qatar

We have already developed a remote experiment laboratory at TAMUQ with an isolated experiment network containing all experimental equipment. All the communications between the Internet enabled devices are delivered through a central server. Figure 5-1 depicts the new isolated experiment network architecture. It consists of

three parts, the client from the Internet, the internal experiment network containing local devices, and a central server.

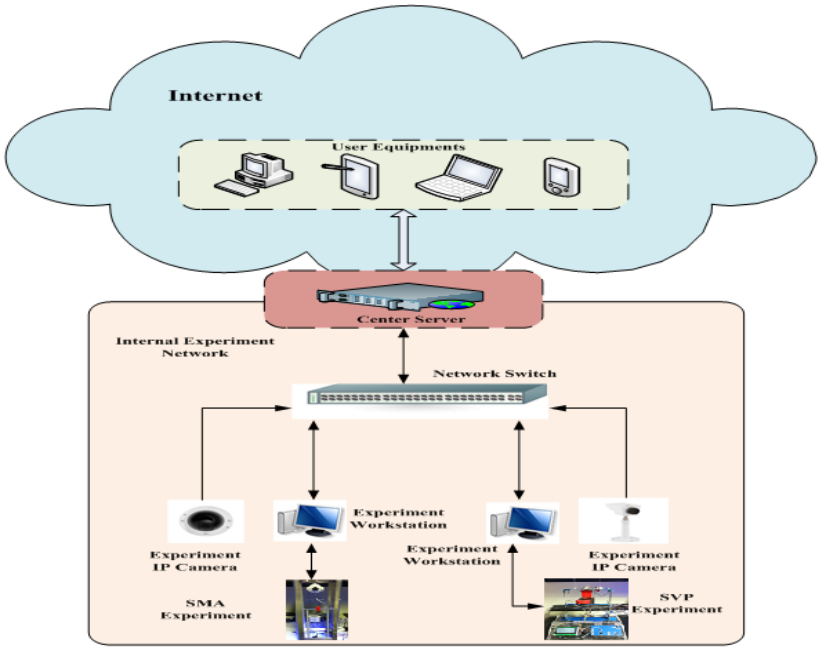


**Figure 5-1:** New isolated experiment network architecture

A central server for remote experiments has been installed and configured at TAMUQ. The remote laboratory website is hosted on the server. The link for the website is http://remotelab.qatar.tamu.edu/. Figure 5-2 shows the main page of the TAMUQ Remote Laboratory website.

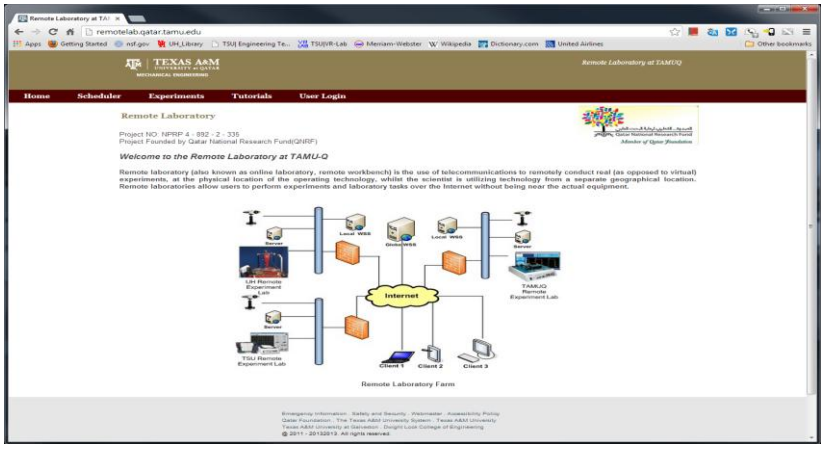


**Figure 5-2:** The main page of the TAMUQ remote laboratory website

We have integrated two experiments into the Remote Laboratory at TAMUQ. As shown in Figure 2-5 and Figure 4-2, the two experiments are Smart Vibration Platform (SVP) experiment and Shape Memory Alloy (SMA) experiment. Figure 5-3 shows the local devices in the remote laboratory at TAMUQ.

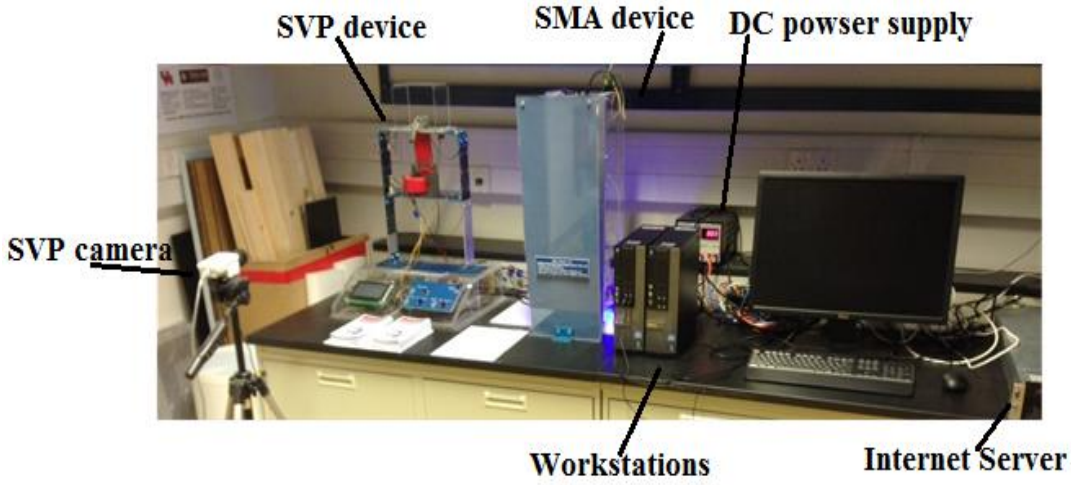


**Figure 5-3:** Local devices in the remote laboratory at TAMUQ

For a real experience in conducting the remote experiments, the users are able to view the experiment through two real-time cameras. One camera for SVP device is placed in front of the device fixed on a camera tripod and the other one for SMA experiment is installed on the back side of SMA device. The modal of two cameras are Axis M1114 for SVP device (Figure 5-4) and Axis M3005V for SMA device (Figure 4-2).

There are two workstations hosting two experiments one by one, as shown in Figure 5-3. Both workstations are installed with LabVIEW 2012 (32-bit). Three DAQ 6008 USB connect to two workstations where two for SVP device and one for SMA device. Programmed VI in LabVIEW running in the workstations controls the experiments. The workstations connect to the central server in a local network. LtoN module in LabVIEW exchanges the experimental data and commands with the server.

Only the server (Figure 5-3) communicates with the Internet. All other devices connect to the server in a local network through a Power over Ethernet (PoE) switch. Four Ethernet cables connect four local devices with the PoE switch and one Ethernet cable connects PoE with the server.

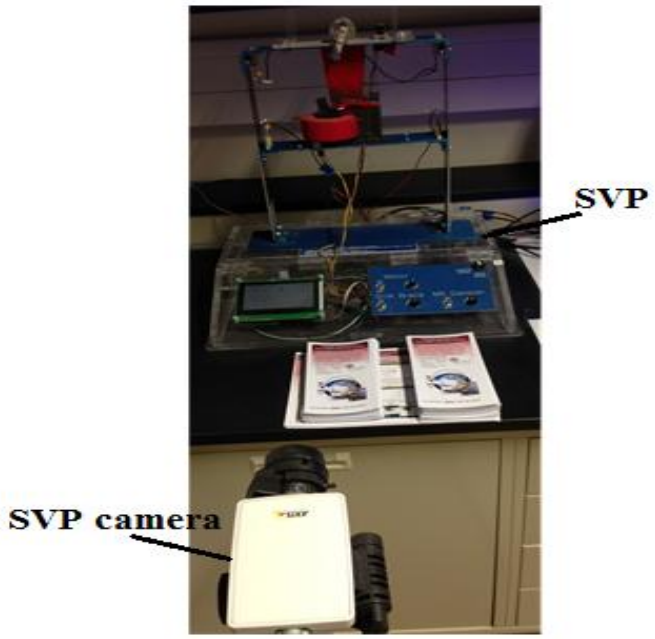


**Figure 5-4:** SVP experiment and camera

## 5.3 New Unified Framework Development

The new unified framework includes three parts: new protocol (LtoN) used in experiment control application to exchange the data and control commands between the experiment workstation and the central server; the Web 2.0 technology for the client application and the server-based Mashup technology for the determination and generation of the user interface (solved by Mr. Ning Wang [56]); and a novel assembled server engine scheme for the server application (Solved by Mr. Ning Wang [56]). The new unified framework was developed and set up under the cooperation among TAMUQ, RSMSL lab at UH and team from TSU.

### 5.3.1 Experiment Control Application

The experiment control application uses Web Service technology to exchange data and commands between the experiment and the central server. LabVIEW to Node.js (LtoN) module is a new real-time protocol using Socket.IO and JSON for the real-time communication between the experiment workstation and central server. Socket.IO is a JavaScript library running in client-side and server-side (Node.js). In order to let the LabVIEW and the server to work together, either LabVIEW has to decode JSON sent from the server (Node.js) or the server has to decode the information from LabVIEW. By taking the advantage of a JSON Tool kit released by NI for LabVIEW, the LtoN module can be developed. By using LtoN, LabVIEW can encode the experimental data in JSON format and send that to the server (with Node.js) as shown in Figure 5-5; decode the commands coming from the server in JSON format and control the experiment according to the commands as show in Figure 5-6. Thus, the real-time exchange of experimental data and commands becomes possible. Figure 5-7 shows the LtoN connection setting in LabvIEW. Table 5-1 depicts the protocol and technology used in the experiment control application.

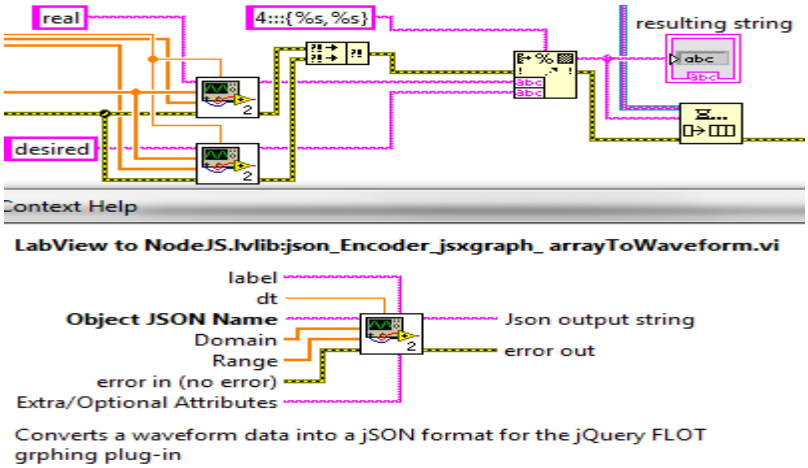


**Figure 5-5:** Data encoder to encode the data into JSON format and send to the server

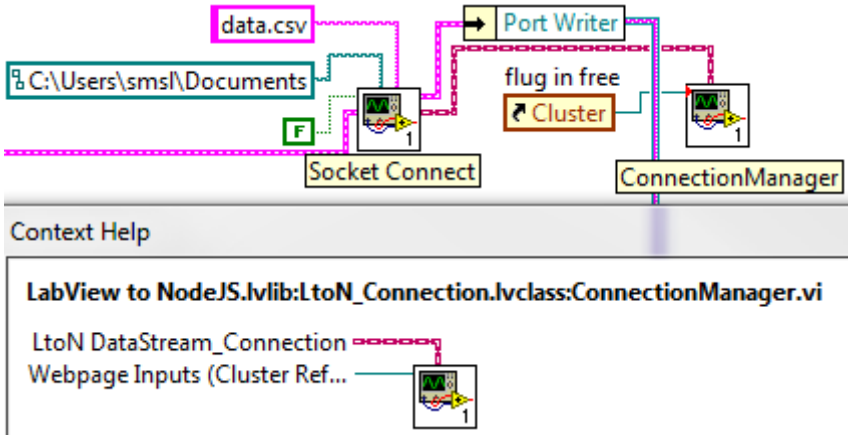


**Figure 5-6:** Control commands decoder to decode JSON from the server

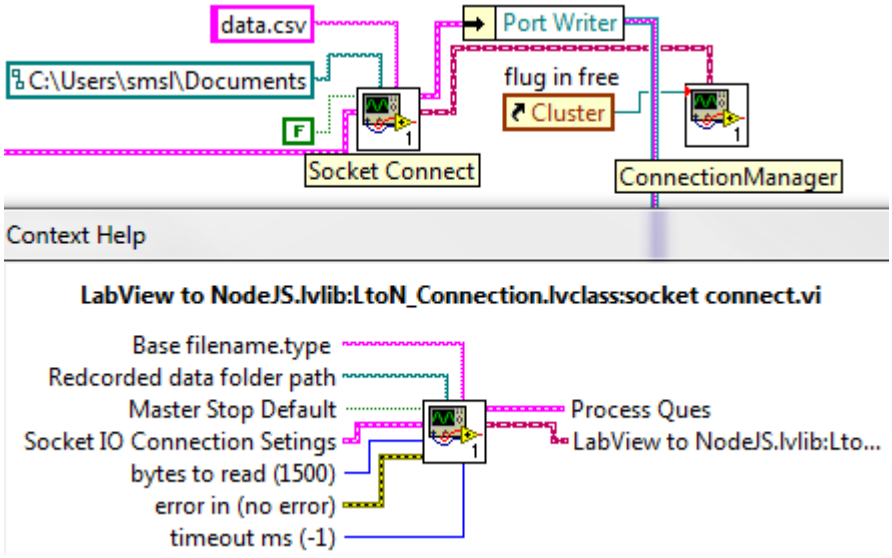


**Figure 5-7:** Socket.IO connection setting module (LtoN) in LabVIEW

**Table 5-1:** Technology/protocol/software list for the experiment control application

| Name | Technology/Protocol/Software | Remark |
|---|---|---|
| Experiment equipment control | LabView (Version 8.6) | |
| Real-Time experiment data communication Module | LabVIEW to Node.js (LtoN) | A new experiment data transmission protocol based on Socket.IO |

### 5.3.2 Client Application and User Interfaces

Client application and user interfaces part is solved by Mr. Ning Wang [56]. In order to manage the remote experiments, we developed a new scalable experiment scheduler system and a new user management system. We used PHP language to implement the

systems, and used MySQL 5.5 database management system to manage the experimental data, user information and other system information. Figure 5-5 shows the screenshots of the scheduler, the experiment conflict control and the experiment management page. The users can use the new interface with all functions without firewall issue.

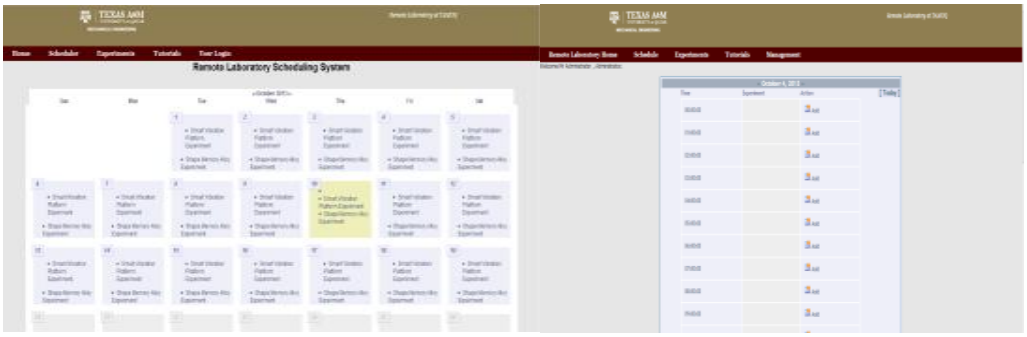

**(a)** Scheduler **(b)** Experiment conflict control

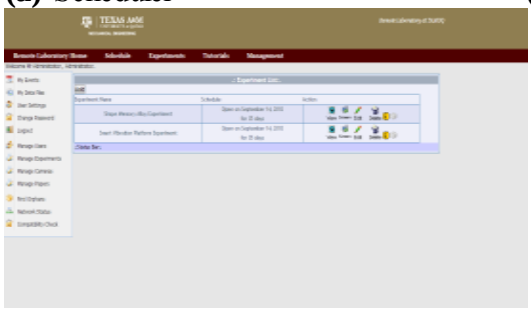

**(c)** Experiment management

**Figure 5-8:** Screenshots of scheduler, experiment conflict control and experiment management page

The Web 2.0 technology and the server-based Mashup technology are used for the client application. The Web 2.0 technology, which includes HyperText Markup Language (HTML), Cascading Style Sheets (CSS), and JQuery/Jquery-Mobile JavaScript libraries, are used to implement the client web application. Table 5-2 lists the technology, protocol and software used in the client web application. The server-based Maship technology is used to generate the user interface. It analyzes and formats the data on a remote server, and transmits the data in a final form to the user's browser. Figure 5-6

depicts three examples of the client application in the remote control of the SMA experiment. This technology allows the users to conduct the experiments in any device, including desktop, smart phones, and other portable devices. Figure 5-7 depicts the novel experiment user interface of controlling the SVP experiment in desktop, iPhone, and iPad.

**Table 5-2:** Technology/protocol/software list for the client web application

| Name | Technology/Protocol/Software | Remark |
|---|---|---|
| Development Language | HTML , CSS, JavaScript | Using HTML5 |
| Real-Time communication Protocol | Socket.IO | Part of Node.js |
| Integration technology | Mashup technology | |
| Widgets | JQuery/ JQuery-Mobile | |

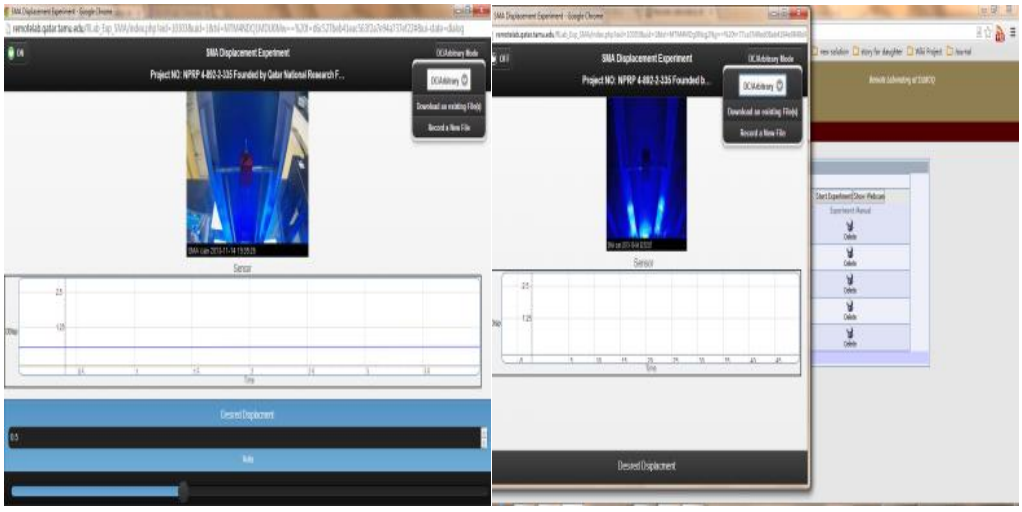


**(a)** User control interface **(b)** Experiment management interface

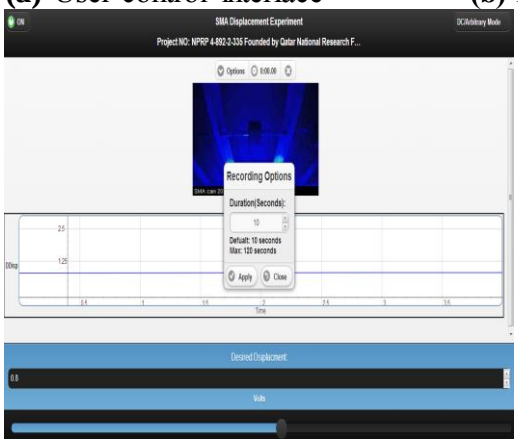


**(c)** Data recording

**Figure 5-9:** Screenshots of SMA experiment user interface

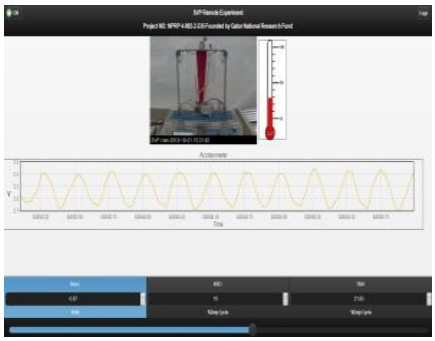

**(a)** User control interface in desktop

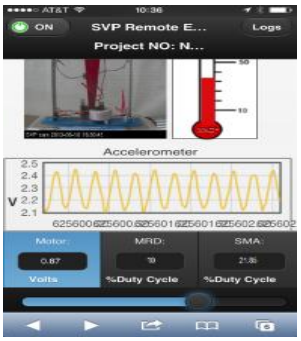


**(b)** User interface in iPhone

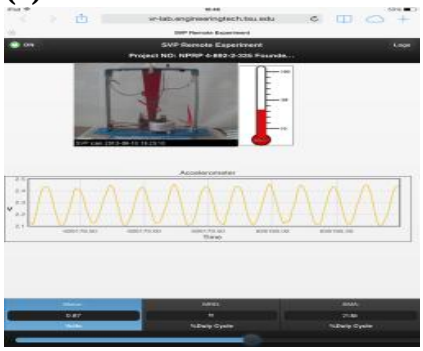

**(c)** User interface in iPad

**Figure 5-10:** The novel experiment user interface of controlling the SVP experiment in desktop, iPhone, and, iPad

The architecture of the Mashup scheme used for the integration of user interface has three layers. Firstly, presentations and user interaction in the user interface of Mashup use HTML, CSS, JAVAScript, and Asynchronous JavaScript. Secondly, in the web services, the system functionality can be accessed by the API services. We use JSON-RPC, REST and SOAP in our novel design. Thirdly, the data is handled in three ways, sending, storing, and receiving. We use JSON and Socket.IO for data transmission.

### 5.3.3 Server Integration

Server integration part is solved by Mr. Ning Wang [56]. The server application is directly built on the top of a novel assembled server engine scheme. It includes two server engines, Apache HTTP server engine and Node.js server engine [54]. Based on the server-based Mashup technology used in the novel framework, the Apache HTTP server

application integrates the user interface widgets with web content and the real-time experiment video, and Node.js server application handles the real-time experiment data transmission. Table 5-3 depicts the technology, protocol and software used in the server application implementation. [55]

**Table 5-3:** Technology/protocol/software list for the server applications

| | Technology/Protocol/Software | Remark |
|---|---|---|
| Server Engine | Apache 2.4.6 , Node.js 0.10.21 | Using the newest stable version |
| Real-Time experiment data Protocol | Socket.IO | Part of Node.js |
| Database | MySQL 5.5 | |
| HTTP Proxy | Node-HTTP-Proxy | Part of Node.js |
| Real-Time video transmission | Http Live Streaming Protocol /FFMPEG /Segmenter software package | |

We implemented the experiment scheduler system and user management system on the server-side. For the data management, we use the MySQL 5.5 Database management system.

## 5.3 Conducting Shape Memory Alloy Experiment Remotely

The SMA experiment can perform arbitrary displacement control as introduced in Chapter four. The function of SMA experiment has been tested remotely by using the novel plug-in free remote laboratory at TAMUQ. The test performed two randomly chosen arbitrary values, 0.932in and 0.646in, as the reference in displacement control. The reference switched between the arbitrary value and zero which was manually control in the GUI. The data containing the real displacement were recorded and were directly downloaded from the GUI. In each test, the GUI was recording the data for 30seconds. Downloading of the data was available in the same GUI. The downloaded data for the real displacement and the displacement reference in each test was plotted in the same

figure by using MATLAB. Figure 5-11 and Figure 5-12 depict the results of the displacement change of SMA in two tests from plug-in free remote laboratory.

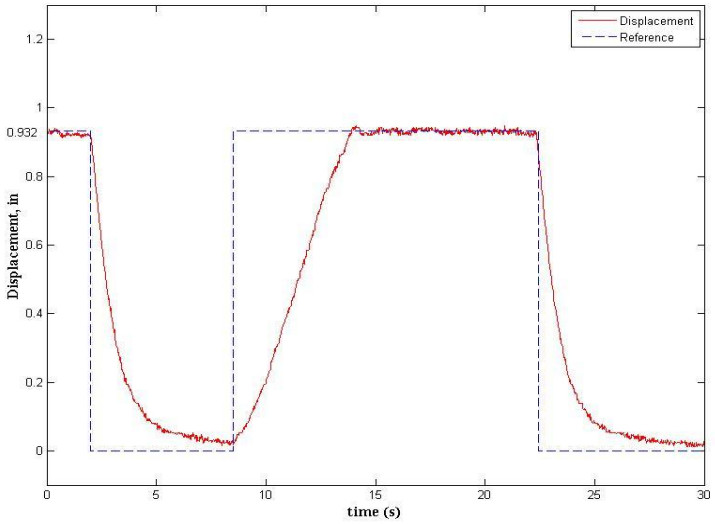


**Figure 5-11:** Arbitrary displacement control (with amplitude of 0.932in) in remote SMA experiment

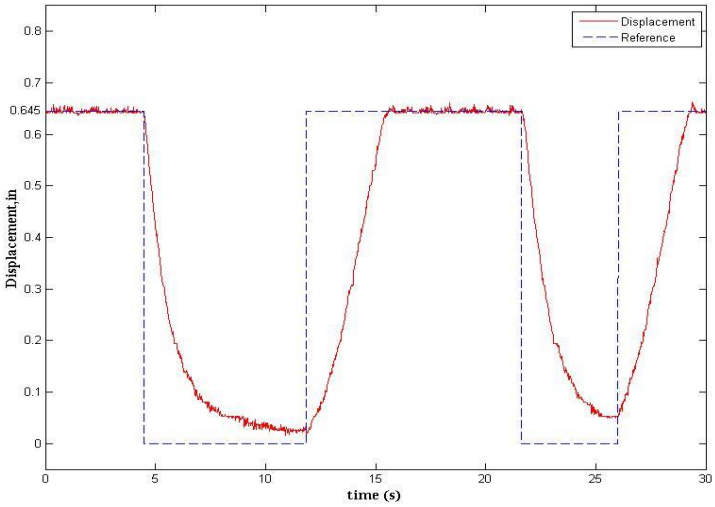


**Figure 5-12:** Arbitrary displacement control (with amplitude of 0.646in) in remote SMA experiment

From Figure 5-13 to Figure 5-15, DC voltage of 6 volts in square waveform with frequencies, 0.01Hz, 0.015Hz, and 0.02Hz, are applied on SMA wire and the

displacement change of SMA are plotted in these figures. At lower frequencies the SMA wire has more time to heat up, the displacement change is larger at lower frequencies.

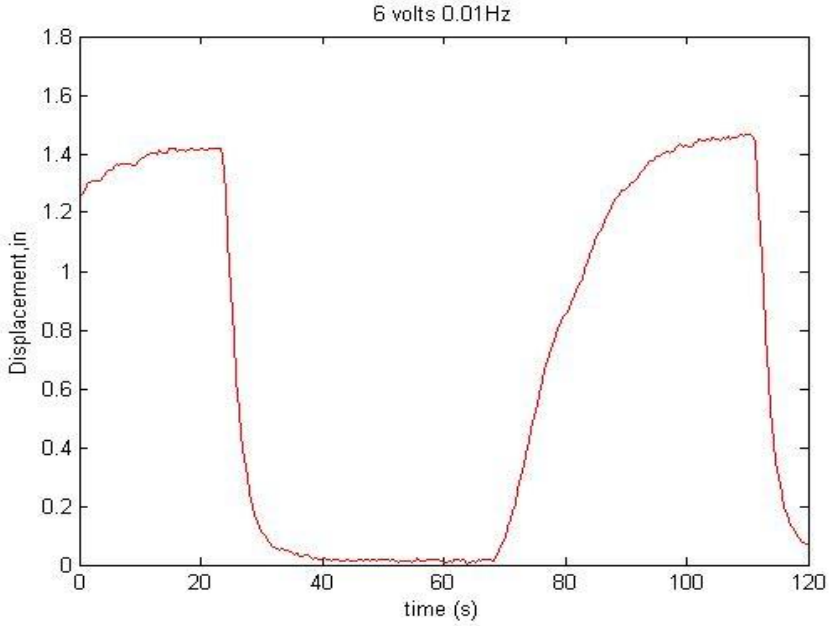


**Figure 5-13:** DC voltage of 6 volts in square waveform applied on SMA wire with frequency of 0.01Hz

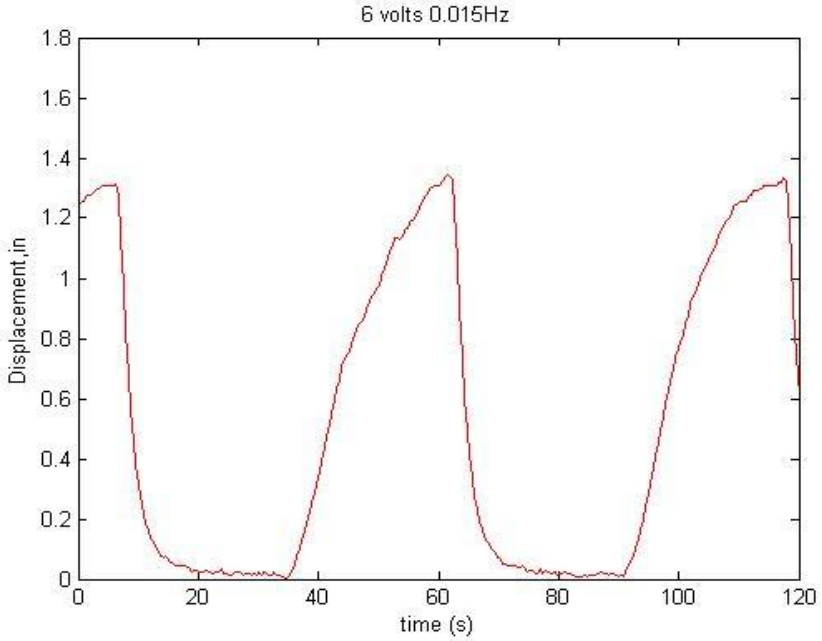


**Figure 5-14:** DC voltage of 6 volts in square waveform applied on SMA wire with frequency of 0.015Hz

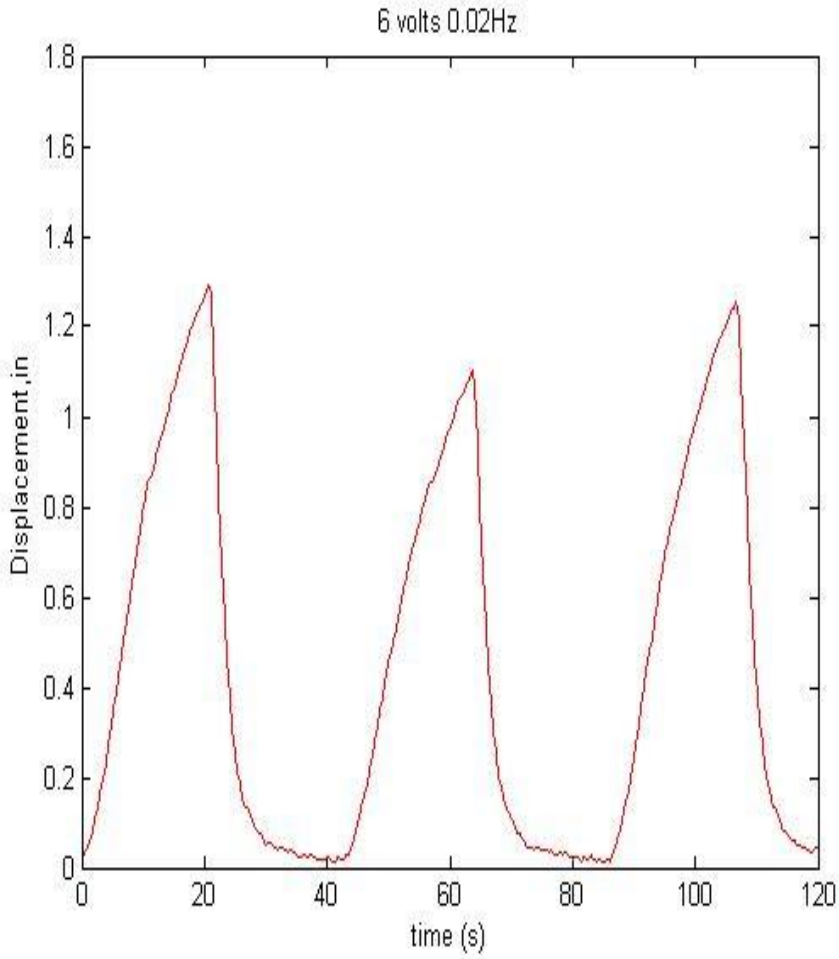


**Figure 5-15:** DC voltage of 6 volts in square waveform applied on SMA wire with frequency of 0.02Hz

The hysteresis of SMA is affected by the frequencies of driving voltage. More demonstrations are performed using AC voltage applied on SMA wire. From Figure 5-16 to Figure 5-33, the displacement change of SMA wire are plotted in both time series and voltage series. Three voltages, 6 volts, 14 volts, and 17 volts, in sinusoidal waveform at frequencies, 0.025Hz, 0.033Hz, and 0.05Hz, are applied on SMA wire. Similar to the results in DC voltage trials, AC voltage at lower frequencies produces more displacement change on SMA wire when the amplitude of voltage keeps the same.

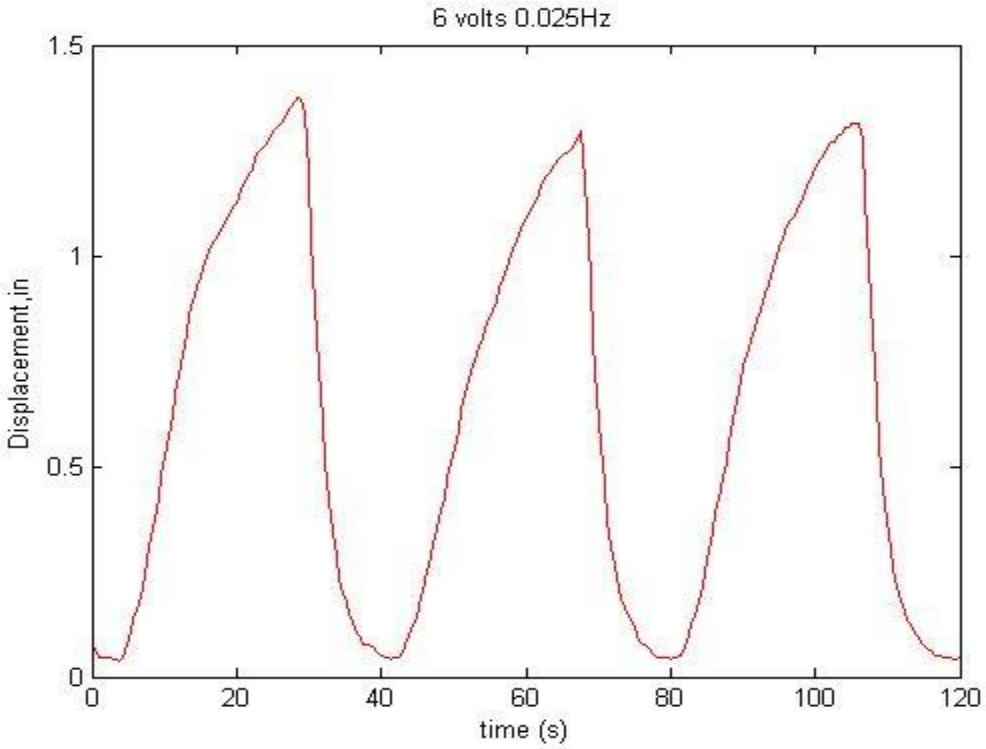


**Figure 5-16:** AC voltage of 6 volts in sinusoidal waveform applied on SMA wire with frequency of 0.025Hz (displacement change in time series)

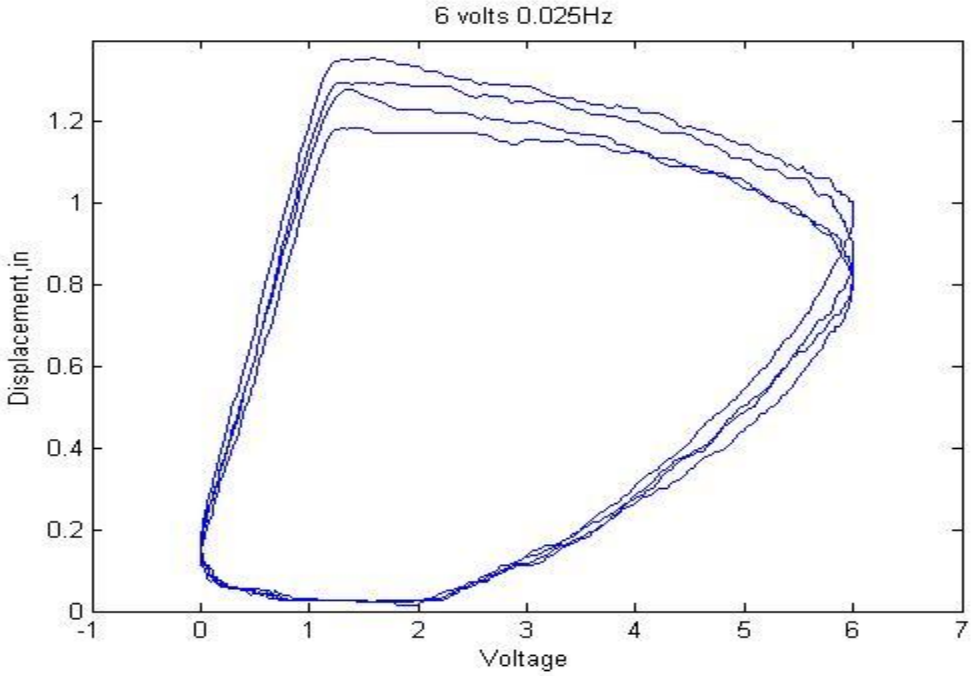


**Figure 5-17:** AC voltage of 6 volts in sinusoidal waveform applied on SMA wire with frequency of 0.025Hz (displacement change in voltage series)

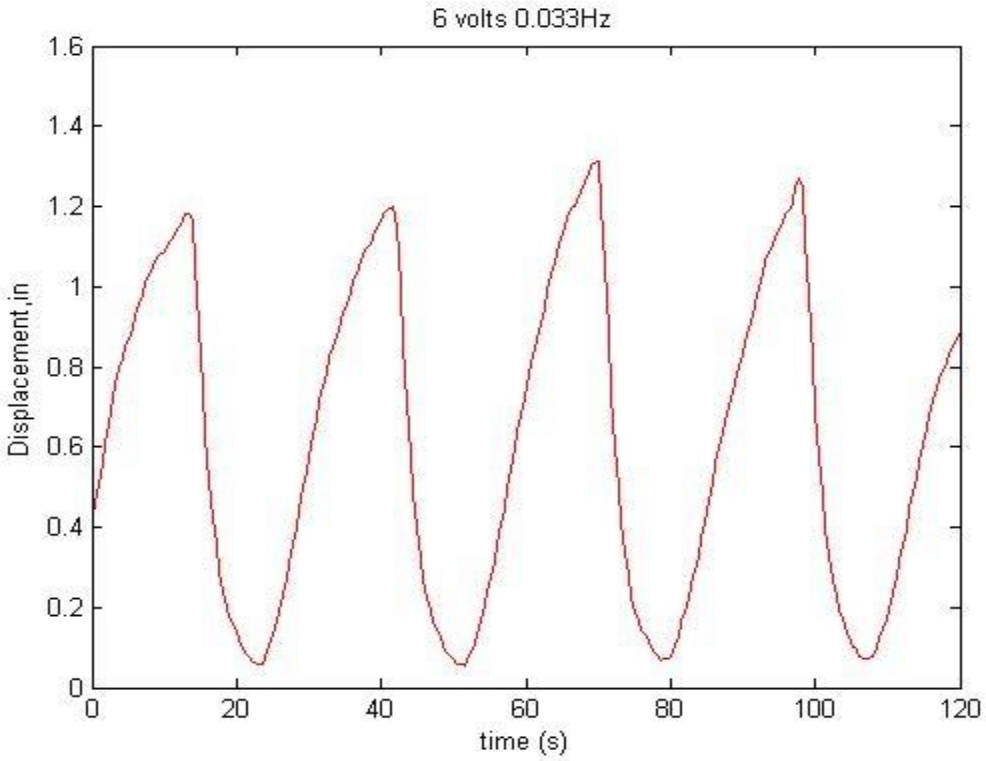


**Figure 5-18:** AC voltage of 6 volts in sinusoidal waveform applied on SMA wire with frequency of 0.033Hz (displacement change in time series)

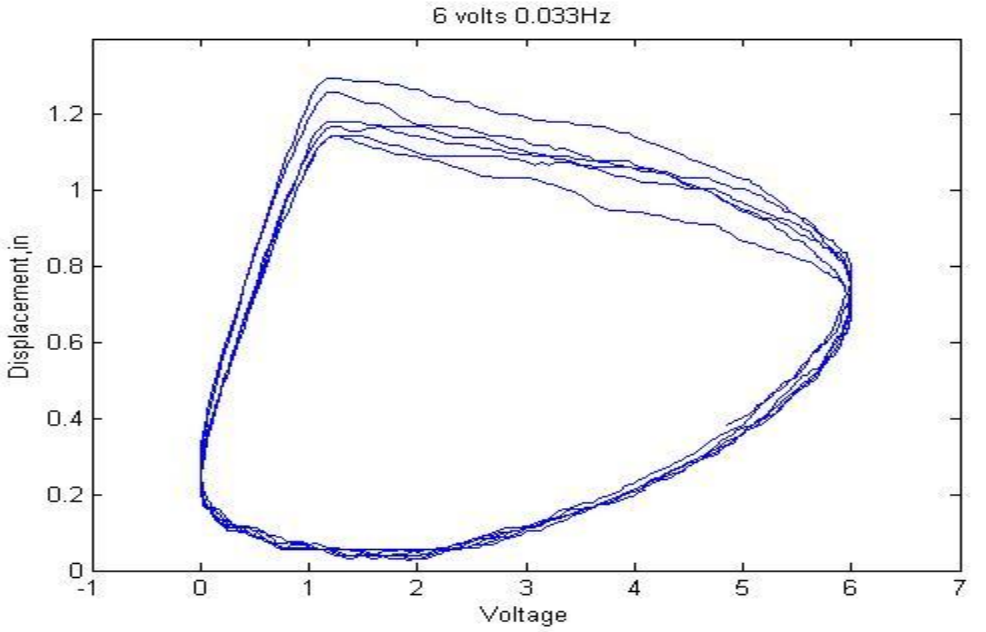


**Figure 5-19:** AC voltage of 6 volts in sinusoidal waveform applied on SMA wire with frequency of 0.033Hz (displacement change in voltage series)

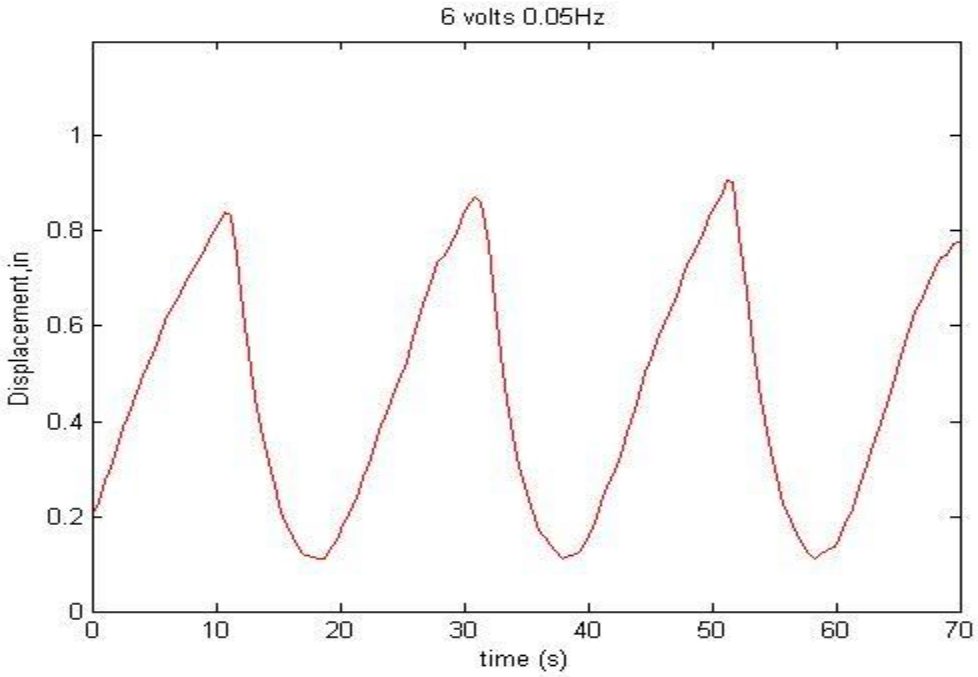


**Figure 5-20:** AC voltage of 6 volts in sinusoidal waveform applied on SMA wire with frequency of 0.05Hz (displacement change in time series)

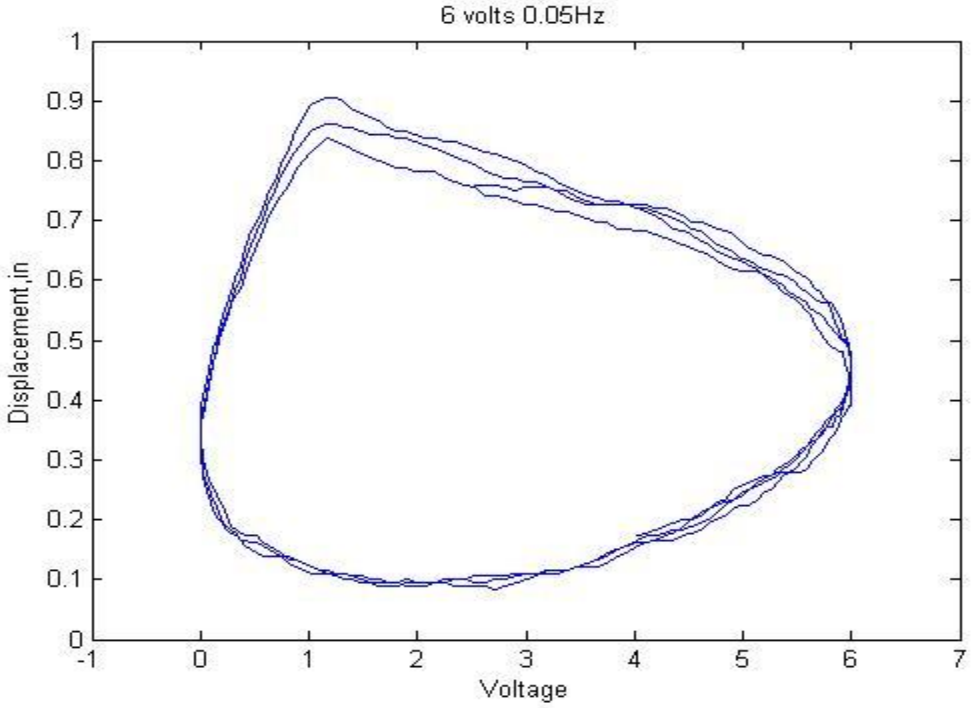


**Figure 5-21:** AC voltage of 6 volts in sinusoidal waveform applied on SMA wire with frequency of 0.05Hz (displacement change in voltage series)

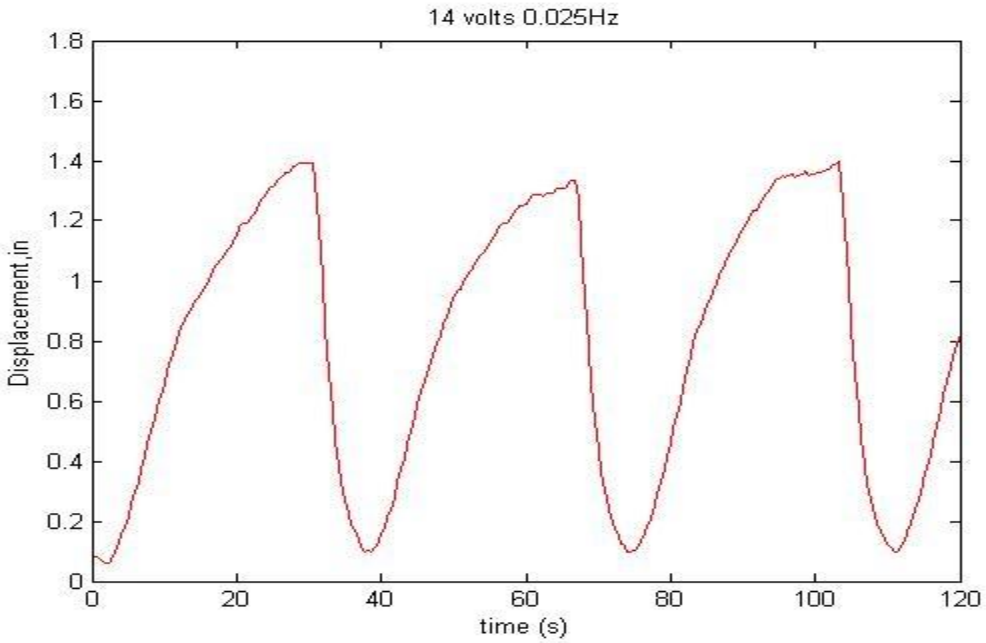


**Figure 5-22:** AC voltage of 14 volts in sinusoidal waveform applied on SMA wire with frequency of 0.025Hz (displacement change in time series)

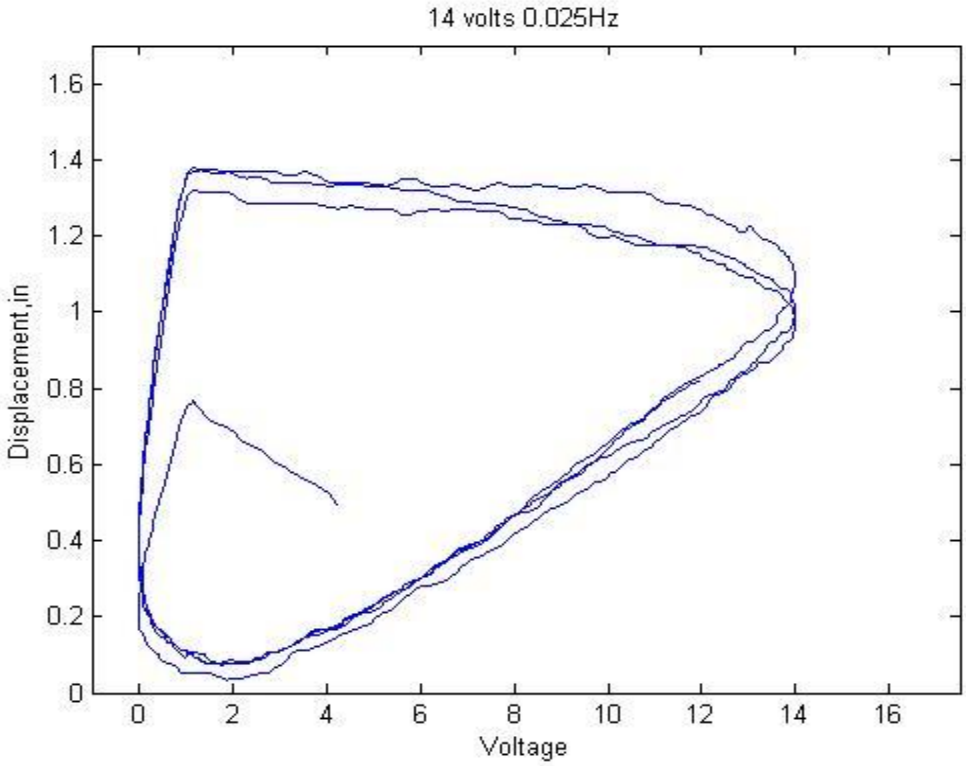


**Figure 5-23:** AC voltage of 14 volts in sinusoidal waveform applied on SMA wire with frequency of 0.025Hz (displacement change in voltage series)

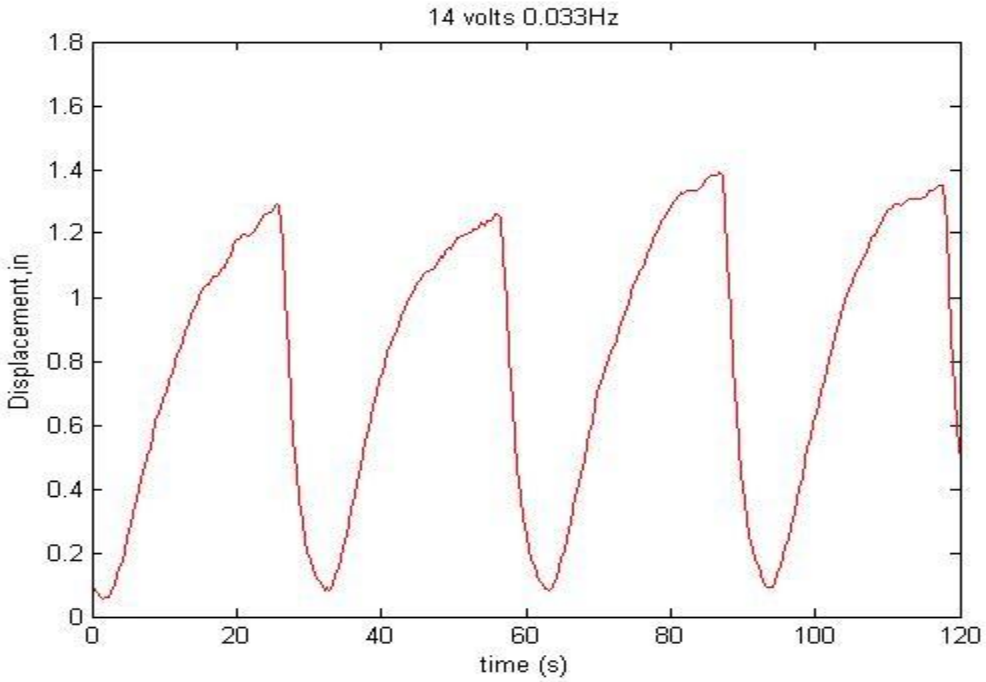


**Figure 5-24:** AC voltage of 14 volts in sinusoidal waveform applied on SMA wire with frequency of 0.033Hz (displacement change in time series)

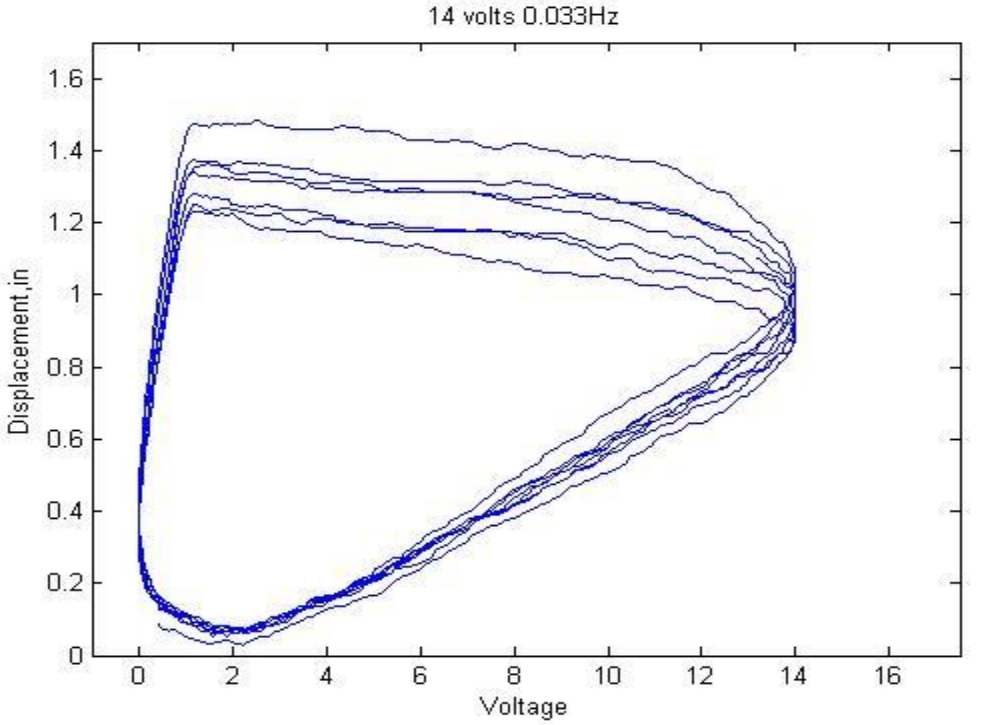


**Figure 5-25:** AC voltage of 14 volts in sinusoidal waveform applied on SMA wire with frequency of 0.033Hz (displacement change in voltage series)

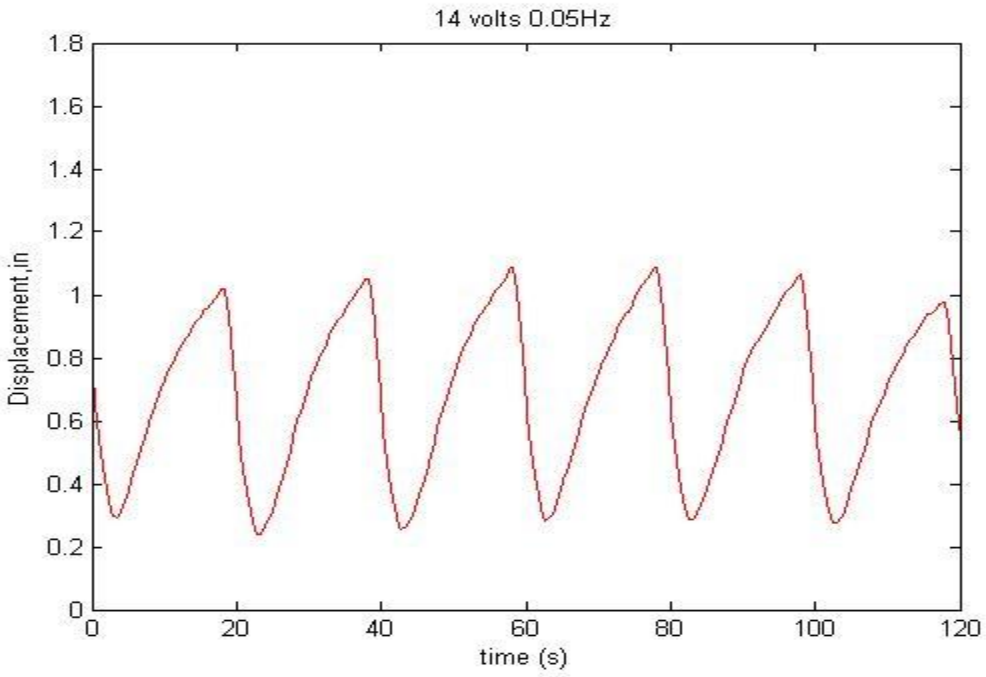


**Figure 5-26:** AC voltage of 14 volts in sinusoidal waveform applied on SMA wire with frequency of 0.05Hz (displacement change in time series)

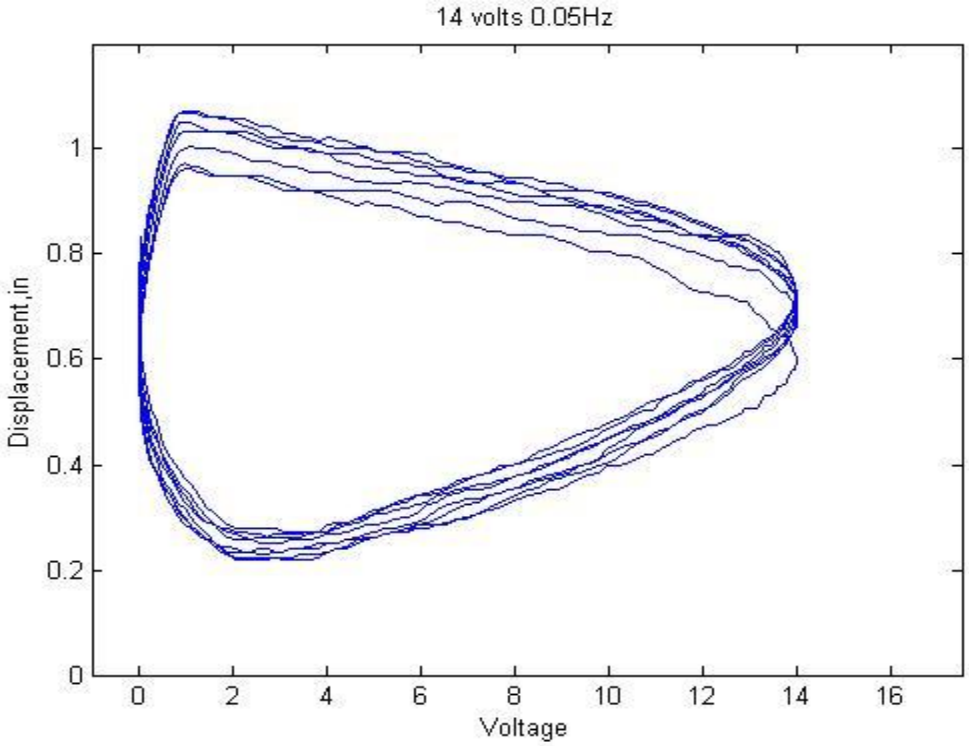


**Figure 5-27:** AC voltage of 14 volts in sinusoidal waveform applied on SMA wire with frequency of 0.05Hz (displacement change in voltage series)

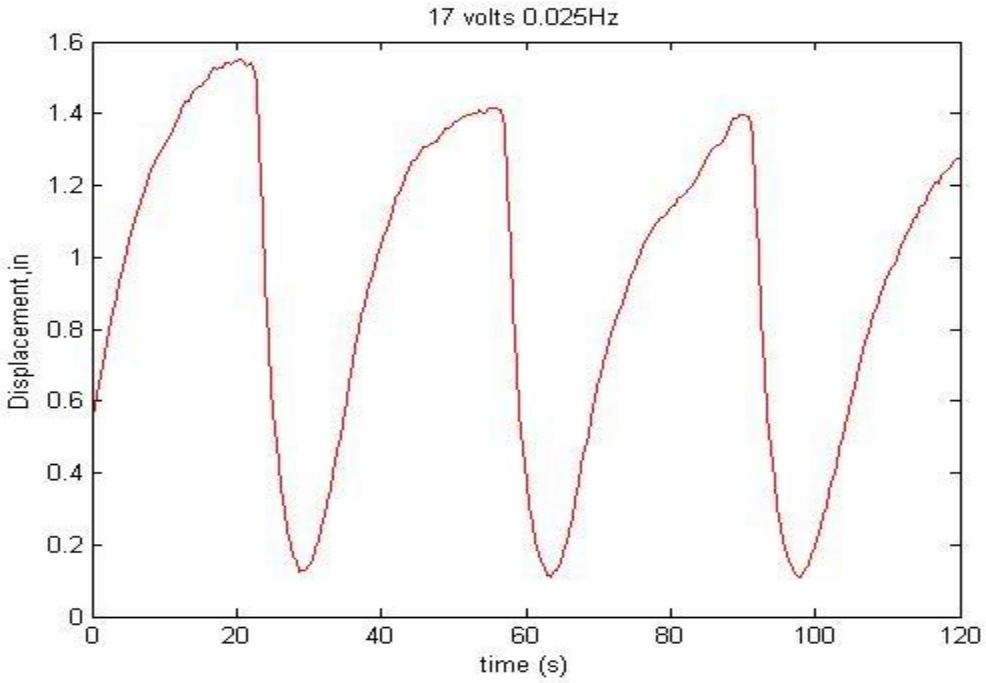


**Figure 5-28:** AC voltage of 17 volts in sinusoidal waveform applied on SMA wire with frequency of 0.025Hz (displacement change in time series)

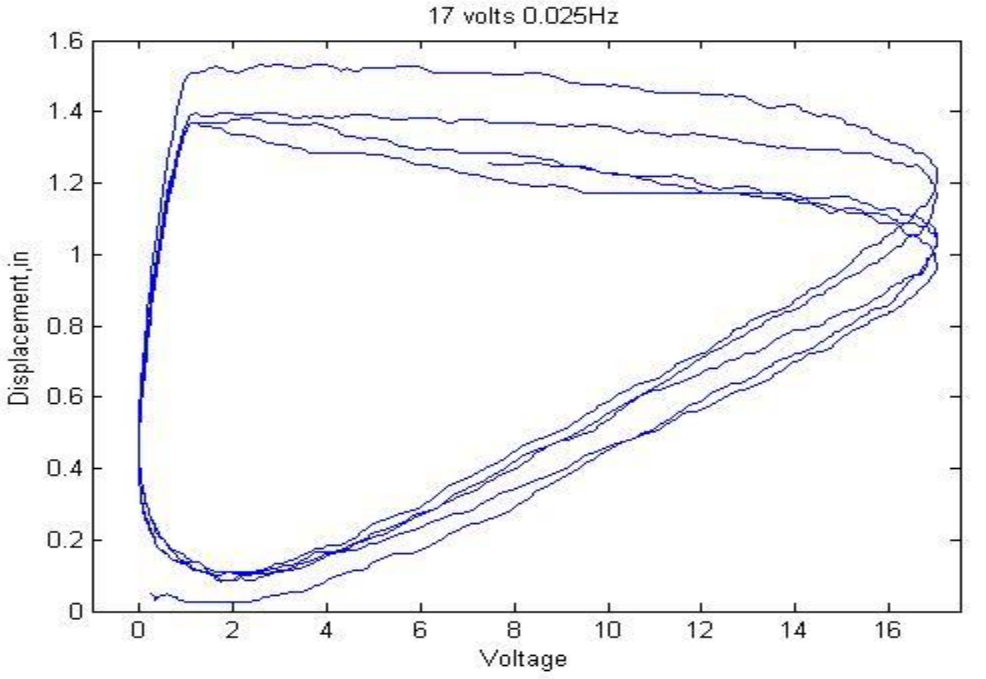


**Figure 5-29:** AC voltage of 17 volts in sinusoidal waveform applied on SMA wire with frequency of 0.025Hz (displacement change in voltage series)

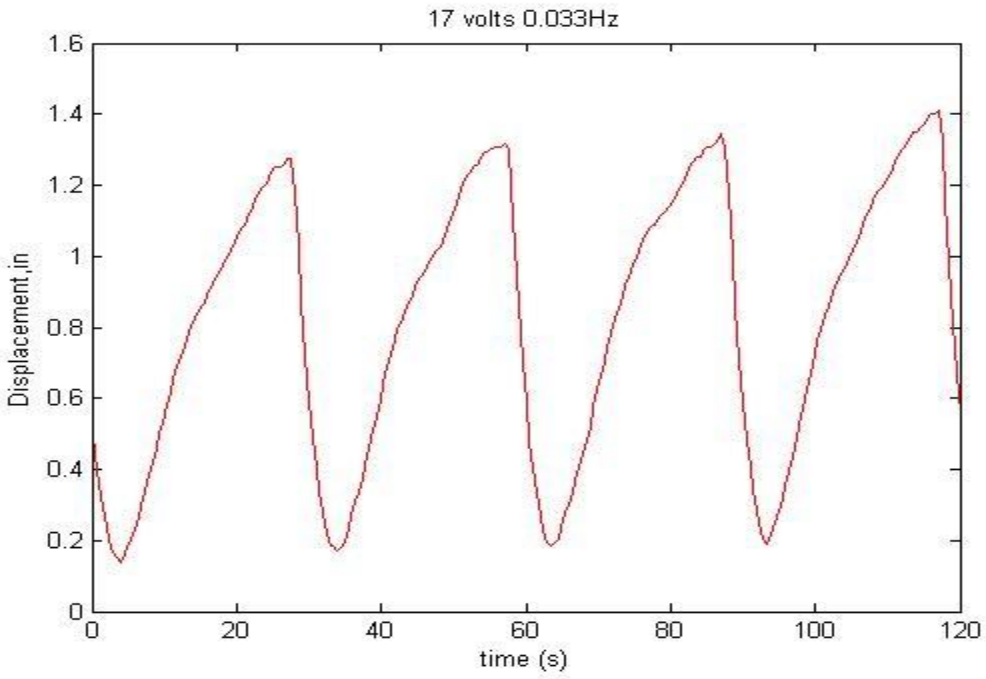


**Figure 5-30:** AC voltage of 17 volts in sinusoidal waveform applied on SMA wire with frequency of 0.033Hz (displacement change in time series)

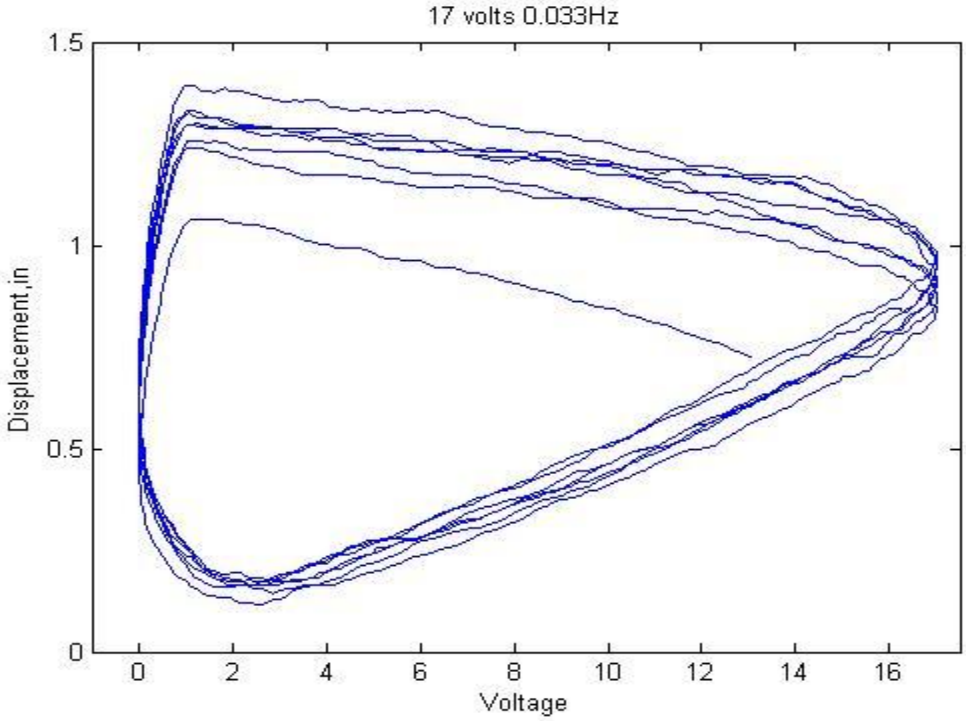


**Figure 5-31:** AC voltage of 17 volts in sinusoidal waveform applied on SMA wire with frequency of 0.033Hz (displacement change in voltage series)

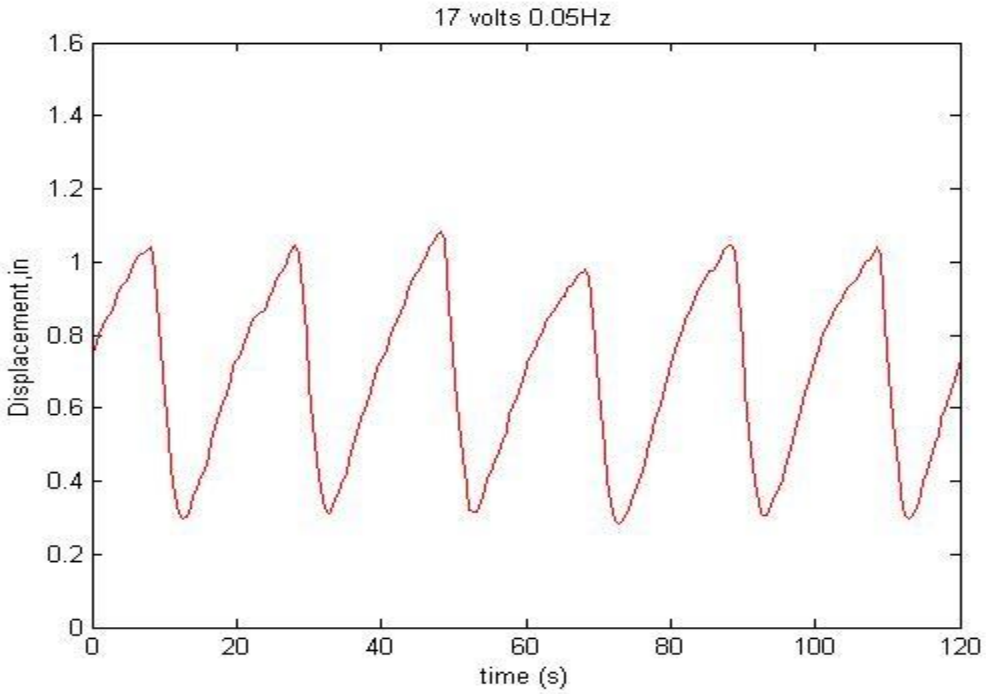


**Figure 5-32:** AC voltage of 17 volts in sinusoidal waveform applied on SMA wire with frequency of 0.05Hz (displacement change in time series)

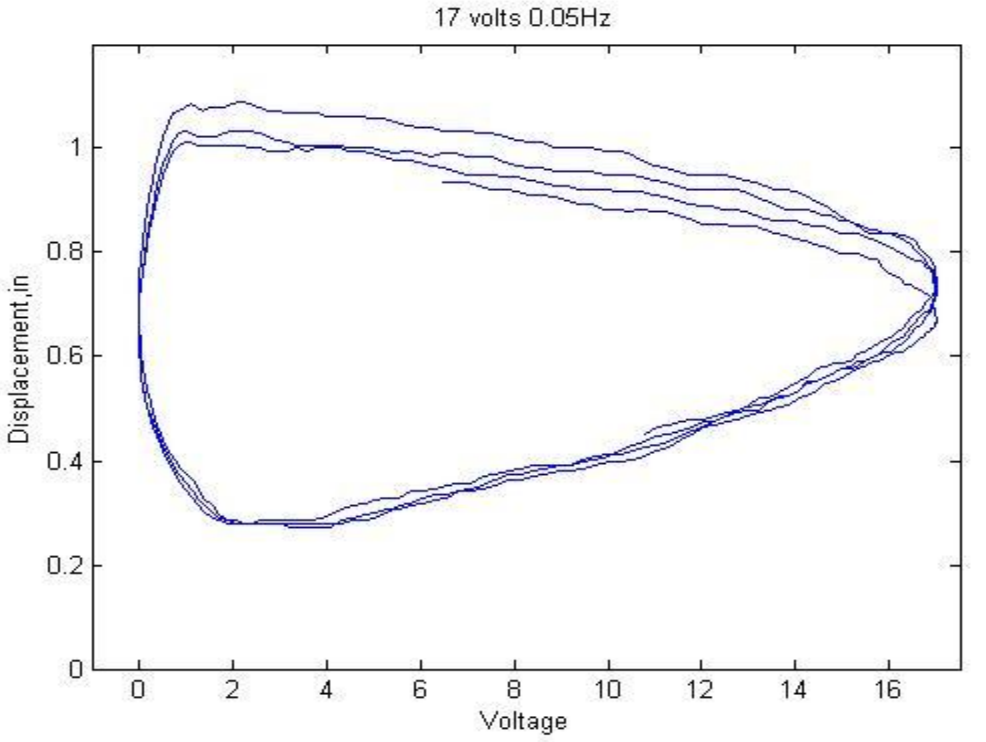


**Figure 5-33:** AC voltage of 17 volts in sinusoidal waveform applied on SMA wire with frequency of 0.05Hz (displacement change in voltage series)

The data collected from the plug-in free remote laboratory has no big difference to the data recorded locally using LabVIEW except for the amplitude of the reference. The amplitude can be different because they are defined by the users. The data recorded from the plug-in free GUI has fewer samples per second comparing to that in local SMA experiment. The data transmission in the GUI is limited to 140 samples per second to minimize the memory and increase the connection speed. In local SMA experiment, the sampling rate is 1000 samples per second; however, by comparing from Figure 5-11 to Figure 5-33 with the experimental results presented in Chapter 4, the hysteresis of SMA has been successfully demonstrated by the data recorded in the plug-in free remote experiment which matches the original results collected locally.

## 5.4 Comparison with the Remote Laboratory Based on LabVIEW Remote Panel

### 5.4.1 Remote Laboratory Based on LabVIEW Remote Panel

Several versions of LabVIEW have furthered the ability to develop distributed applications: TCP/IP, Internet Toolkit, VI Server, Front Panel Web Publishing, Remote Data Acquisition (RDA), DataSocket, and so on [55]. In addition, several third party toolkits have enabled internet-based VI control: LabVNC and AppletVIEW. Then, of course, there has always been PC Anywhere and other similar applications that provide general remote control of a PC. With enough effort, you can create distributed applications using these tools. However, each one presents unique challenges, often requiring advanced programming techniques and development of custom data handling mechanisms. It provides users to LabVIEW remote panels. One of the first things in LabVIEW application development is that VI consists of front panels, diagrams, and

behind the scenes, compiled executable code. Furthermore, these components are always bound together for a VI that is executing. The front panel and compiled code have both been required for operating a front panel.

The SMA experiment based on LabVIEW has its own remote panel, as shown in Figure 5-34. This is a similar SMA experiment previously developed by RSMSL at UH. The remote panel in LabVIEW can be easily created in the VI application. Once the programming in LabVIEW is done, users can use Web Publishing Tool to create a website for remote control. In order to run the remote panel to control the real VI application, users need to install LabVIEW run-time engine in their computer. The following Figure depicts a LabVIEW remote panel used in traditional version of remote lab at UH. This remote panel is displayed in a web browser and the users can use it as they are using LabVIEW. In this remote lab, users are able to perform voltage control, position control and temperature control through the web remotely on the real experiment. The data, in terms of temperature, voltage and displacement, are displayed in this panel too. The same data in addition to time and temperature can be saved remotely to the server by the data saving feature in LabVIEW. Those data are available for downloading from the RSMSL Remote Laboratory website.

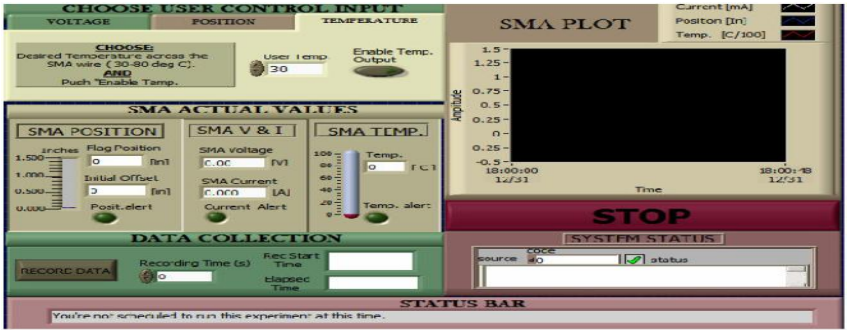


**Figure 5-34:** SMA experiment LabVIEW Remote Panel

Table 5-4 compares the differences between the remote control of VI in LabVIEW remote panel and the local control of VI in LabVIEW. The front panel of VI can be controlled in two ways, remotely through the remote panel or directly in LabVIEW in the workstation. LabVIEW remote panel is a powerful tool which will enable many programmers to create distributed applications easily.

**Table 5-4:** Comparison between the remote control using the LabVIEW remote panel and the local control of VI in LabVIEW

| | LabVIEW Remote Panel | LabVIEW VI Control |
|---|---|---|
| Run the VI | Only the LabVIEW run-time Engine and browser plug-in are required on the client machine. The LabVIEW development environment is not requirement | The LabVIEW environment (or a LabVIEW executable with a menu option to run remote panels) and LabVIEW run-time are required. A web browser is not required. |
| Connection | The browser allows connecting to the local program on the same machine as the server.(http://localhost/name of (the VI.html)) | Connecting to the remote panel from LabVIEW on the same machine as the server is not permitted. |
| Control | Only the "operate" menu is available in browser's remote panel. | Regular LabVIEW menu options are available with certain items disabled. |
| HTML File | An HTML file must be created to control remote panel in the web browser. Once the HTML page is created, any changes to the front panel are automatically reflected in the remote panel viewed in the web browser. | An HTML page is not required. |

### 5.4.2 Comparison between the LabVIEW Based Remote Laboratory and the Novel Remote Laboratory as Presented

With the remote panel in LabVIEW, users can operate the front panel on a machine that is separate from where the VI resides and executes. Furthermore, they can embed the front panel into a web page and operate it within that page. The client machine needs a browser and the LabVIEW runtime engine and other browser plug-ins. Because the

installation of runtime engine and other plug-ins have limitations, our novel plug-in free remote laboratory is desired. The novel remote laboratory can be used in any portable devices and any workstations with browser and the Internet.

The novel remote panel has three advantages plug-in free, no firewall issue and compatible to any system and any devices. The users can use a web browser without any firewall issue to operate the experiment through their devices including smart phones and tablets. The user interface is plug-in free because JavaScript used in the development of GUI is a common and widely used programming language. Regular web browsers are good to use all the features of the novel remote panel without any issue including the real-time video.

## 5.5 Summary

The novel remote laboratory with the new unified framework has been developed at TAMUQ. There are two remote experiments, SMA experiment and SVP experiment, integrated into the novel remote laboratory. The new remote laboratory has several advantages comparing to the regular LabVIEW-based remote laboratory. The novel remote laboratory is plug-in free and compatible to any system, browsers, and devices including tablets and smart phones. Real-time videos are available for the users to view the experiments at the same time of conducting the experiments. The development of the novel remote laboratory will benefit the engineering education in TAMUQ at Qatar. In the future, we are able to add more remote experiments to the novel remote laboratory and link three remote laboratories at UH, TSU, and TAMUQ into one farm of remote laboratories.

# Chapter 6 Conclusion and Future Work

In the last two decades, the engineering education community has carried out numerous initiatives to develop and implement remote laboratory for engineering education. Smart materials have many applications and implementation in research and industries. We successfully developed a remote laboratory with the Novel Unified Framework and integrated two remote experiments of using smart materials SMA and MR fluids into the remote laboratory in TAMUQ at Qatar. The remote laboratory with the Novel Unified Framework is plug-in free, without firewall issue and compatible to any devices and smartphones.

In Chapter 2, we had a general review on the state of the art about remote laboratory and also the remote laboratory set up at the University of Houston. In addition, we reviewed the SVP device used in the remote laboratory at TAMUQ, which was developed and built by other students at UH and TAMUQ. We also covered the nonlinear feedback control method of SMA and compared three conventional robust controllers, bang-bang compensator, saturation compensator, and smooth compensator, for the feedback control of SMA.

In Chapter 3, we had a general review on smart materials and discussed SMA and MR fluids in detail. SMA is shape-memory materiel and MR fluid is field-dependent material. SMA can return to its original shape by heating it up to let SMA to change from Martensite phase to Austenite phase. Atomic arrangement changes in the phase change recovered the original shape of SMA. SMA has hysteresis in the phase transformation which makes SMA nonlinear in the feedback control. SMA is a popular material to use as actuators for various purposes. We also had a general review of MR fluids. MR fluids

change from liquid state to semi solid state in the presence of magnetic field. It has many advantages comparing to other field-dependent materials like ER fluids. MR fluids roughly follow Bingham model in the presence of magnetic field and become Newtonian fluids in the absence of magnetic field. The shear stress of MR fluids is dependent on the applied magnetic field. Many applications like shock absorbers, brakes, and dampers use MR fluids.

In Chapter 4, we introduced the SMA device for the remote SMA experiment. SMA experiment helps the student to learn the hysteresis of SMA and the effects from the frequency change in driving voltage on the hysteresis loop. The remote SMA experiment uses programmed NI LabVIEW VI to control the experiment and also the data exchange between the workstation and the web central server. The experiment has application of sliding mode based feedback control and smooth robust compensator to control the displacement of SMA. The implementations of displacement control and voltage applied on SMA use PWM method and SSR. PWM method controls the experiment by switching the electric circuit on/off based on the feedback of SMA. SSR is a hardware providing possible swift on/off switches in the electric circuit. Finally, the SMA experiment successfully demonstrates the hysteresis of SMA and the hysteresis change affected by the frequency change of driving voltage as shown in the results of the experiment.

In Chapter 5, we covered the novel remote laboratory with the Novel Remote Framework. A remote laboratory with the new unified framework has been set up at TAMUQ. There are two remote experiments, SVP experiments and SMA experiments, integrated into the remote laboratory. The remote laboratory has a website, http://remotelab.qatar.tamu.edu, for the users to schedule experiments and conduct the

experiments remotely. The experiments use LabVIEW VI in their control and the data communication between the experiments and the server uses LabVIEW to Node.js (LtoN) module. We also compared the remote laboratory with the novel remote laboratory to the regular LabVIEW-based remote laboratory. The novel remote laboratory is plug-in free and real-time videos are available for the users to view the experiments without firewall issue. The users can control the remote experiments in any system and any devices including tablets and smartphones by using the novel remote laboratory.

The novel remote laboratory with new unified framework is scalable. We are able to add more remote experiments to the remote laboratory using the same technologies. The development of the remote laboratory at TAMUQ is aim to benefit the engineering education for the students at TAMUQ. In the future, three remote laboratories at UH, TSU, and TAMUQ are able to combine into one by integrating all the remote experiments to the novel remote laboratory with new unified framework. By doing so, we can share all the sources and save the efforts and cost of managing three remote laboratories separately.

## References


[1] X. Chen, C. Olmi, and G. Song, "A Remote Bridge Experiment with Vibration Control," *In Proceedings of International Symposium of Life-Cycle Performance of Bridges and Structures*, pp844-849, Changsha, China, June, 2010

[2] G. Song and P. Lam, "Improve Teaching of System Dynamics and Response Using Smart Material Experiment," *Journal of Science Mathematic Engineering Technology Education: Innovations and Research*, vol. 2/3&4 September-December, pp. 11-18, 2001.

[3] R. M. Felder and L. K. Silverman, "Learning and teaching styles in engineering education," *Engineering of Education*, vol. 78, pp. 674-681, 1988

[4] B. J. Furman and G. P. Hayward, "Asynchronous Hands-on Experimetns for Mechatronics Education," Mechatronics, *Elsevier Science Ltd*, vol. 12, pp. 251-260, 2002.

[5] C. Gravier, J. Fayolle, B. Bayard, M. Ates and J. Lardon, " State of the Art about Remote Laboratories Paradigms – Foundations of Ongoing Mutations," *International Journal of Online Engineering,* Vol. 4, Issue 1, pp. 19-25, February, 2008.

[6] V. J. Harward, J. A. Delalamo, S. R. Leerman, P. H. Bailey, J. Carpenter, K. Delong, C. Felknor, J. Hardison, B. Harrison, I. Jabbour, P. D. Long, T. Mao, L. Naamani, J. Northridge, M. Schulz, D. Talavera, C. Varadharajan, S. Wang, K. Yehia, R. Zbib and D. Zych, "The iLab Shared Architecture: A Web Services Infrastructure to Build Communities of Internet Accessible Laboratories," *Proceedings of the IEEE*, Vol. 96, No.6, June 2008.

[7] M. T. Restivo, J. Mendes, A. M. Lopes, C. M. Silva, and F. Chouzal, "A Remote

Laboratory in Engineering Measurement," *Industrial Electronics, IEEE Transactions on,* Vol. 56, pp. 4836-4843, 2009.

[8] R. Pastor, J. Sanchez and S. Dormido, "Web-based Virtual Lab and Remote Experimentation Using Easy Java Simulations," *16th IFAC World Congress,* Vol. 16, Part 1, pp. 2289, 2005.

[9] P. Bistak,"Remote Laboratory Server Based on Java Matlab Interface," *14th International Conference on Interactive Collaborative Learning (ICL 2011)*, pp. 344-347, 2011.

[10] A. Melkonya, A. Gampe, M. Pontual, G. Huang and D. Akopian, "Facilitating Remote Laboratory Deployments Using a Relay Gateway Server Architecture," *IEEE Transactions on Industrial Electronics,* Vol. 61, No. 1, Jan. 2014.

[11] P. Bailey and J. Hardison, "iLab Batched Experiment Architecture: Client and Lab Server Design," *MIT iCampus iLabs Software Arch. Workshop,* June 13-15, 2006.

[12] V.Mateos, A. Gallardo, T. Richter, L. Bellido, P. Debicki and V. Villagra, "LiLa Booking System: Architecture and Conceptual Model of a Rig Booking System for On-Line Laboratories," *International Journal of Online Engineering,* Vol. 7, Issue 4, Nov. 2011.

[13] D. Lowe, S. Murray, E. Lindsay and D. Liu, "Evolving Remote Laboratory Architectures to Leverage Emerging Internet Technologies," *IEEE Transactions on Learning Technologies,* Vol. 2, No. 4, Oct-Dec, 2009.

[14] Duro, N., Dormido, R., Vargas, H., Dormido-Canto, S., "An Integrated Virtual and Remote Control Lab: The Three-Tank System as a Case Study," *Computing in Science & Engineering (2008),* 10(4), 50-59.

[15] S. Jeschke, T. Richter and U. Sinha, "Embedding Virtual and Remote Experiments into a Cooperative Knowledge Space," *Paper presented at the 38th ASEE/IEEE Frontiers in Education Conference*, Saratoga Springs, NY, Oct. 2008

[16] Olmi, C., Song, G., & Mo, Y. L., "An innovative and multi-functional smart vibration platform," *Smart Mater. Struct*. (2007), 16, 1302–1309.

[17] G. Song, B. Kelly, and B. N. Agrawal, "Active position control of shape memory alloy wire actuated composite beam," *Smart Materials and Structures*, 9, 711-716.

[18] K. B. Lazarus, E. Saarmaa, G. S. Agnes, "Active smart material system for buffet load alleviation," *Proc. SPIE Smart Structures and Materials: Industrial and Commercial Applications of Smart Structures Technologies, C. R. Crowe and G. L. Anderson, eds.,* vol. 2447. 179-192.

[19] A. Gontean, R. Szabo, and I. Lie, "LabVIEW Powered Remote Lab", 15th *International Symposium for Design and Technology of Electronics Packages*, pp. 335-340, Sept. 17-20, 2009.

[20] C. Olmi, X. Chen, and G. Song, "A Framework for Developing Scalable Remote Experiment Laboratory," *In Proceedings of World Conference on E-Learning in Corporate, Government, Health care and Higher Education 2011*, pp. 2045-2050, Honolulu, Hawaii, Oct. 18-21, 2011.

[21] G. Song, C. Olmi, and R. Bannerot, "Enhancing Vibration and Controls Teaching with Remote Laboratory Experiments", *Proceedings of the 2007 American Society for Engineering Education Annual Conference and Exposition, Honolulu*, Hawaii, 2007.

[22] S. A. Ambrose, and C. H. Amon, "Systematic design of a first-year mechanical

engineering course at Carnegie Mellon University," *Journal of Engineering Education,* 173-181, 1997.

[23] D. Boehringer, S. Jeschke, and T. Richter,"Lila-A European Project on networked Experiments," *Sixth International Conference on Remote Enginnering and Virtual Instrumentation*, 2009.

[24] X. Chen, Y. Zhang, S. Darayan, L. Kehinde, D. Olowokere, and D. Osakue, "Using Virtual and Remote Laboratory to Enhance Engineering Technology Education," *Proc., ASEE Annual Conference & Exposition,* AC 2011-914. Vancouver, BC, Canada, 2011.

[25] X. Chen, L. Jiang, S. Darayan, L. Kehinde, and D. Olowokere, "Technologies for developing of virtual and remote laboratories – a case study," *Proc., ASEE Annual Conference & Exposition. AC 2009-1350*, Austin, TX, 2009.

[26] Song G and Ma N, "Robust Control of a Shape Memory Alloy Wire Actuated Flap," *Smart Mater. Struct.,* Vol., Issue 6, pp. N51-N57, 2007.

[27] S. Majima, K. Kodama and T. Hasegawa T, "Modeling of shape memory alloy actuator and tracking control system with the model," *IEEE Trans. Control Syst. Technol.* Vol. 7, pp. 511-28, 1999.

[28] Fan B and Song G, "Hysteresis in a Shape Memory Alloy Wire: Identification and Simulation," *Conference Proceeding Smart Structures and Materials 2005: Modeling, Signal Processing*, and Control, May 23, 2005.

[29] Song G and Quinn D "Experimental Study of Robust Tracking Control a Shape Memory Alloy Wire Actuator," *Journal of Dynamic Systems, Measurement, and Control,* Vol. 126, Issue 3, p. 674, 2004.

[30] A. Kilicarslan, G. Song and K. Grigoriadis,"ANFIS Based Modeling and Inverse Control of a Thin SMA Wire," *Proceeding of Modeling, Signal Processing, and Control for Smart Structures,* Vol. 6926, Issue 1, 2008.

[31] G. Song and R. Mukherjee, "A Comparative Study of Conventional Non-Smooth Time-Invariant and Smooth Robust Compensator," *Transaction on IEEE, Control Systems Technology,* Vol.6, Issue 4, 1998.

[32] L. Cai and G. Song, " A smooth robust nonlinear controller for robot manipulator with joint stick-slip friction," *Proc. IEEE Int. Conf. on Robotics Autom.,* pp 449-54, Atlanta, GA, 1993

[33] L Cai and A. Abdalla, "A smooth tracking controllers for uncertain robot manipulator," *Proc. IEEE Int. Conf. on Robotics Autom.*, pp. 83-8, Atlanta, GA, 1993

[34] R. Sehab, "Fuzzy PID Supervision for a Nonlinear System: Design and Implementation," *2007 Annual Meeting of the North American Fuzzy Information Processing Society,* pp. 36-41, 2007.

[35] S. Lentijo, S.pytel, A.Monti, J.Hudgins, E.Santi and G.Simin, "FPGA Based Sliding Mode Control for High Frequency Power Converters," *IEEE 35th Annual Power Electronics Specialists Conference,* vol. 5, pp 3588-3592, 2004.

[36] H. Bang, C. Ha and J. H. Kim, "Flexible Spacecraft Attitude Maneuver by Application of Sliding Mode Control," *Acta Astronautica,* Vol. 57, Issue 11, pp. 841-850, 2005.

[37] R. Cepeda-Gomez, N.Olgac and D.A. Sierra, "Application of Sliding Mode Control to Swarms under Conflict," *IET Control Theory and Applications,* Vol. 5, Issue 10, pp. 1167-1175, 2010.

[38] N. T. Tai and K. K. Ahn, "A RBF Neural Network Sliding Mode Controller for SMA Actuator," *International Journal of Control, Automation, and Systems,* Vol. 8, No. 6, pp. 1296-1302, 2010.

[39] H. Kizmaz, S. Aksoy and A. Muhurcu, "Sliding Mode Control of Suspended Pendulum," *Modern Electric Power Systems,* pp1-6, 2010.

[40] G.K. Lowe and M.A. Zohdy, "Modeling Nonlinear Systems Using Multiple Piecewise Linear Equations," *Nonlinear Analysis: Modeling and Control,* vol. 15, no. 4, pp. 451-458, 2010.

[41] G. Song, "Intelligent Structural Systems," University of Houston, Class Notes 2013.

[42] N. Shatrova , "Heating of a shape memory alloy spring," from University of Cambridge DoIYPoMS Teaching and Learning Packages, http://www.doitpoms.ac.uk/ldplib/shape_memory/printall.php.

[43] R. AlSaleh, F. Casciati, A. El-Attar and I EL-Habbal, "Experimental Validation of a Shape Memory Alloy Retrofitting Application," *Journal of Vibration and Control,* vol. 18, Issue 1, pp. 28-41, 2011.

[44] C. Chrysostomou, A. Stassis, T. Demetriou and K. Hamdaoui, "Application of shape memory prestressing devices on an ancient aqueduct," *Smart Structures and Systems,* Vol. 2, pp. 261-278, 2008.

[45] R. W. Phillips, "Engineering Applications of Fluids with a Variable Yield Stress", Ph. D. Thesis, University of California, Berkeley (1969).

[46] K. D. Weiss, J. D. Carlson and D. A. Nixon, "Viscoelastic Properties of Magneto- and Electro- Rheological Fluids," *J. Intell. Mater. Syst. And Struct.* Vol. 5, pp. 772-775, 1994.

[47] M. Nakano, H. Yamamoto and M.R. Jolly, "Dynamic Viscoelasticity of a Magnetorheological Fluid in Oscillatory Slit Flow," *6th Int. Conf. On ERF, MRS and Their Applications*, 22-25 July, 1997, Yonezawa, JP (1997).

[48] C. Kormann, M. Laun and G. Klett *Actuator 94, 4th Int. Conf. On New Actuators*, eds. H. Borgmann and K. Lenz, Axon Technologies Consult GmbH, 271 (1994).

[49] D. Grant and V. Hayward, "Variable structure control of shape memory alloy actuator," *IEEE Control syst. Mag.,* vol. 17, pp. 80-8, 1997

[50] F. Vasca, L. Lannelli, Dynamics and Control of Switched Electronic Systems Advanced Perspectives for Modeling, Simulation and Control of Power Converters, p492, 2012.

[51] S. R. Bowes and S. Grewal, "Modulation strategy for single phase PWM inverters," *Electron. Lett*., vol. 34, no. 5, pp. 420-422, Mar.5, 1998.

[52] M. A. Boost and P. D. Ziogas, " State-of-the-art carrier PWM techniques: A critical evaluation," *IEEE Trans. Ind. Appl.,* vol. 24, no. 2, pp. 271-280, Mar./Apr. 1988.

[53] H. S. Black, "Modulation Theory," Van Nostrand Reihnold, New York (1953).

[54] Hughes-Croucher, T. and Wilson, M., Up and Running with Node.js (First ed.), O'Reilly Media (April, 2012), p. 204, ISBN 978-1-4493-9858-3.

[55] J. Weng, N. Wang, X. Chen, G. Song, and H. Parsaei, "Development of a Remote SMA Experiment- A Case Study," University of Houston and Texas Southern University, 2014.

[56] N. Wang, "Design and Implementation of the Advanced Technology for Remote Laboratory," the Master of Science Degree thesis in Texas Southern University, Houston, Texas, 2014.